THE JOURNAL OF COMPARATIVE NEUROLOGY 369:571–590 (1996)

Differential Glutamatergic Innervation in Cytochrome Oxidase-Rich and -Poor Regions of the Macaque Striate Cortex: Quantitative EM Analysis of Neurons and Neuropil

FENG NIE AND MARGARET T.T. WONG-RILEY
Department of Cellular Biology and Anatomy, Medical College of Wisconsin, Milwaukee, Wisconsin 53226

ABSTRACT

One of the hallmarks of the primate striate cortex is the presence of cytochrome oxidase (CO)-rich puffs and CO-poor interpuffs in its supragranular layers. However, the neurochemical basis for their differences in metabolic activity and physiological properties is not well understood. The goals of the present study were to determine whether CO levels in postsynaptic neuronal compartments were correlated with the proportion of excitatory glutamate-immunoreactive (Glu-IR) synapses they received and if Glu-IR terminals and synapses in puffs differed from those in interpuffs. By combining CO histochemistry and postembedding Glu immunocytochemistry on the *same* ultrathin sections, the simultaneous distribution of the two markers in individual neuronal profiles was quantitatively analyzed. As a comparison, adjacent sections were identically processed for the double labeling of CO and GABA, an inhibitory neurotransmitter. In both puffs and interpuffs, most axon terminals forming asymmetric synapses (84%)—but not symmetric ones, which were GABA-IR—were intensely immunoreactive for Glu. GABA-IR neurons received mainly Glu-IR synapses on their cell bodies, and they had three times as many mitochondria darkly reactive for CO than Glu-rich neurons, which received only GABA-IR axosomatic synapses. In puffs, GABA-IR neurons received a significantly higher ratio of Glu-IR to GABA-IR axosomatic synapses and contained about twice as many darkly CO-reactive mitochondria than those in interpuffs. There were significantly more Glu-IR synapses and a higher ratio of Glu- to GABA-IR synapses in the neuropil of puffs than of interpuffs. Moreover, Glu-IR axon terminals in puffs contained approximately three times more darkly CO-reactive mitochondria than those in interpuffs, suggesting that the former may be synaptically more active. Thus, the present results are consistent with our hypothesis that the levels of oxidative metabolism in postsynaptic neurons and neuropil are positively correlated with the proportion of excitatory synapses they receive. Our findings also suggest that excitatory synaptic activity may be more prominent in puffs than in interpuffs, and that the neurochemical and synaptic differences may constitute one of the bases for physiological and functional diversities between the two regions.

Indexing terms: glutamate immunocytochemistry, CO histochemistry mitochondria, puff, interpuff

The anatomical organization of the primate striate cortex displays highly ordered patterns in its extrinsic and intrinsic neural connectivity that obeys clear laminar and columnar boundaries, within which neurons sharing similar physiological properties tend to be grouped together (Hubel and Wiesel, 1962, 1969, 1972; Lund, 1990). One of the hallmarks of the macaque striate cortex is the presence of regularly repeating puff-like structures (or blob) in its supragranular layers, as revealed by cytochrome oxidase, a mitochondrial energy-generating enzyme (Hendrickson et al., 1981; Horton and Hubel, 1981; Wikstrom et al., 1981; Wong-Riley and Carroll, 1984). The intense CO activity reflects a heightened level of neuronal activity in puffs as

Accepted January 19, 1996.

Please address reprint requests to Dr. Margaret Wong-Riley, Department of Cellular Biology and Anatomy, Medical College of Wisconsin, 8701 Watertown Plank Road, Milwaukee, Wisconsin 53226.

compared to the surrounding regions, the interpuffs (Livingstone and Hubel, 1984a; Wong-Riley, 1989, 1994; DeYoe et al., 1995). Physiologically, puffs differ from interpuffs in their higher levels of spontaneous activity and their lack of orientation selectivity (Livingstone and Hubel, 1984a; Ts'o and Gilbert, 1988). Anatomically, the two regions receive input from discrete sources and participate in different projections, implying that the synaptic innervation to these regions may differ (Livingstone and Hubel, 1982, 1984b; Fitzpatrick et al., 1983). Recently, it has become increasingly clear that puffs also differ chemically from interpuffs in the distribution and levels of neurotransmitters and their receptors (Fitzpatrick et al., 1987; Hendry et al., 1987, 1990, 1994; Kuljis and Rakic, 1989; Hendry and Carder, 1992; Carder and Hendry, 1994; Wong-Riley, 1994). These findings suggest the need for further investigations into the neurochemical and synaptic organization of puffs and interpuffs, specifically in relationship to the metabolic and physiological diversities between the two regions. Indeed, much of the cortical microcircuitry appears to be governed by rules that apply to both excitatory and inhibitory synaptic transmission (Lund, 1990; Tsumoto, 1990).

Recently, we started to address this issue by studying the distribution of inhibitory GABAergic and nonGABAergic synapses in puffs and interpuffs, and its relationship with CO levels in postsynaptic neuronal compartments (Nie and Wong-Riley, 1995). We found that CO-rich puffs received a higher proportion of nonGABAergic synapses, which were presumed excitatory based on their morphological features, than CO-poor interpuffs (Gray, 1959; Uchizono, 1965; Wong-Riley et al., 1989b; Nie and Wong-Riley, 1995). At the cellular level, GABAergic neurons, which are consistent with type C cells previously classified, received mainly nonGABAergic synapses on their cell bodies and they contained a much higher CO level than nonGABA neurons (type A and type B cells) that received exclusively GABAergic axosomatic synapses (Wong-Riley et al., 1989a, 1994; Nie and Wong-Riley, 1995). These results strongly suggest that the differences in metabolic levels and physiological properties among various neuronal groups and between puffs and interpuffs may depend on the differential synaptic innervation they receive, as indicated by the asymmetric distribution of inhibitory and presumed excitatory synapses. However, it is still not known whether these nonGABAergic presynaptic axon terminals are chemically excitatory.

Following the finding of a strong excitatory effect of glutamate on cortical neurons (Curtis and Watkin, 1963; Krnjevic and Phillis, 1963), a substantial body of evidence suggested that glutamate was involved in cortical transmission (Baughman and Gilbert, 1980; Watkins and Evans, 1981; Storm-Mathisen et al., 1983; Fonnum, 1984; Hicks, 1987; Conti et al., 1988, 1989; Storm-Mathisen and Ottersen, 1988; Montero and Wenthold, 1989; Montero, 1990). Glutamate is transported into axonal terminals by a high-affinity, sodium-dependent uptake system, concentrated in synaptic vesicles, and released following depolarizing stimuli. The reversal potentials of iontophoretically applied glutamate and synaptically evoked responses were similar in the cerebral cortex and spinal cord neurons (Balcar and Johnson, 1972; de Belleroche and Bradford, 1972; Nadler et al., 1977; Toggenburger et al., 1982). Based on these findings, glutamate is considered to be a major excitatory synaptic transmitter in the CNS, acting on diverse ionotropic and second messenger-coupled receptors (Mayer and Westbrook, 1987; Hollman et al., 1989; Monaghan et al., 1989; Tsumoto, 1990; Moriyoshi et al., 1991). More recently, immunohistochemical studies in the macaque striate cortex at the light microscopic level indicated that the patches of intense glutamate immunoreactivity, largely representing presumed axon terminals, coincided with regions of CO-rich puffs, whereas light immunostained regions matched CO-poor interpuffs (Carder and Hendry, 1994). These results suggest that the distribution of glutamatergic axon terminals and synapses may be different between puffs and interpuffs. However, verification of this issue will require quantitative analysis with glutamate immunocytochemistry at the electron microscopic (EM) level.

The major purpose of the present study was to test the hypothesis that the level of oxidative metabolism as revealed by CO activity in postsynaptic neurons and neuropil of puffs and interpuffs is positively correlated with the proportion of excitatory glutamatergic synapses they receive. To reach this goal, we devised a double labeling technique combining CO histochemistry and postembedding glutamate or GABA immunocytochemistry on the *same* ultrathin sections. CO activity, indicated by CO histochemistry, served as a marker for the level of oxidative capacity. Postembedding immunocytochemistry was used to examine the subcellular distribution of glutamate and to identify Glu-IR synaptic terminals in puffs and interpuffs. Adjacent sections were equally processed by double labeling for CO and GABA and were compared with those stained for CO and glutamate. This novel technique is necessary in the present study for several reasons: First, puffs and interpuffs are too small and closely spaced to be dissected accurately without CO histochemistry; second, only the double labeling technique can simultaneously reveal CO and glutamate on the *same* section at the ultrastructural level. By using this technique, we wished to determine whether 1) presumed excitatory axon terminals that were nonGABA-IR contained a high level of glutamate in puffs and interpuffs; 2) CO levels in postsynaptic neurons were correlated with the proportion of Glu-IR to GABA-IR axosomatic synapses they received; and 3) Glu-IR axon terminals and synapses in puffs differed from those in interpuffs. A preliminary report of our findings was presented elsewhere (Nie et al., 1994).

MATERIALS AND METHODS

Animal and tissue preparation

Three adult macaque monkeys (*Macaca mulatta*) were used in this experiment. Animals were deeply anesthetized with ketamine HCl (25 mg/kg, i.m.) and sodium pentobarbital (35 mg/kg, i.p.). They were perfused via the left ventricle with warm 0.1M sodium phosphate-buffered saline followed by cold (4°C) fixative consisting of 2.5% paraformaldehyde, 1.5% glutaraldehyde, and 4% sucrose in 0.1 M sodium phosphate buffer, pH 7.35. The brains were promptly removed and placed in the cold fixative for 1 hour followed by three rinses in the original buffer. For EM analysis, 60-μm vibratome sections from the exposed opercular striate cortex away from the foveal representation (but within the central 10°) were cut in the tangential plane. They were reacted for CO histochemistry as previously described (Wong-Riley, 1979).

The reacted vibratome sections were viewed under a dissecting microscope, and core samples of puffs and interpuffs in layer III were taken with a modified No. 25 gauge

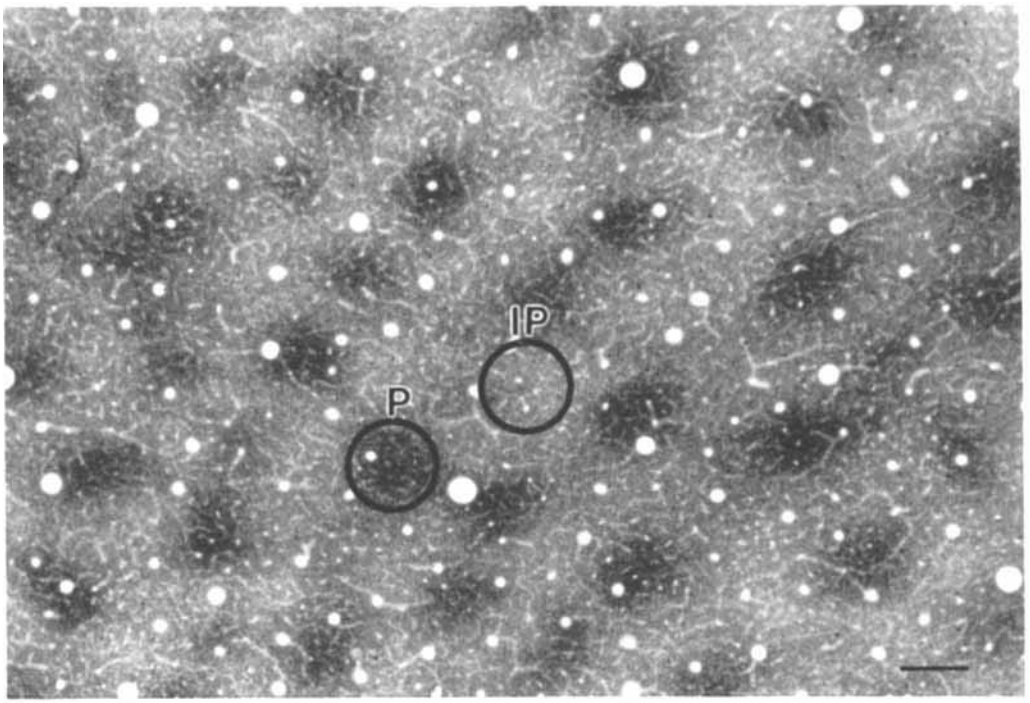

Fig. 1. A cytochrome oxidase (CO)-reacted vibratome section showing CO-rich puffs (circle, P) and CO-poor interpuffs (circle, IP). Under a dissecting microscope, these zones can be easily distinguished, and core samples were taken from either puffs or interpuffs. The opposite side of each section was also checked to insure that the entire core sample was confined to either a puff or an interpuff, and any sample crossing over both regions was discarded. Scale bar = 100 μm.

hypodermic needle. Figure 1 shows that puffs and interpuffs can be clearly distinguished on CO-reacted vibratome sections. After each dissection, the opposite side of the section was checked to ensure that the entire core sample was taken only from either a puff or an interpuff. Any sample crossing over both regions was discarded to ensure their accurate localization. The samples were postfixed for 1 hour in 1% osmium tetroxide in 0.1 M phosphate buffer (PB), pH 7.35, at 4°C. They were washed again in PB and dehydrated in a graded series of alcohol. The sections were then embedded in a resin (Durcupan ACM, Fluka), and cured for 72 hours at 56°C.

Postembedding immnocytochemistry for glutamate

Ultrathin sections of CO-reacted puffs or interpuffs were cut and picked up on Formvar-coated, single slot, nickel grids for postembedding glutamate immunocytochemistry. The following procedures of Somogyi and Soltesz (1986) with minor modifications (Nie and Wong-Riley, 1995) were used for postembedding glutamate immunocytochemistry. Ultrathin sections were treated with 2% aqueous solution of sodium metaperiodate for 20 minutes and rinsed three times in distilled water. They were then placed in Tris (10 mM)-phosphate (10 mM)-buffered isotonic saline, pH 7.6, containing 1% NGS (TPBS) and 0.1 % Triton X-100 for 30 min. Grids were then transferred to drops containing the glutamate-antisera (Arnel) diluted 1:4000 in the same TPBS buffer. The incubation time in the primary antisera was 4 hours at room temperature (RT). Afterwards, sections were rinsed three times in TPBS and then incubated in the secondary antibodies (goat antirabbit IgG conjugated to 15 nm colloidal gold, Amersham) diluted 1:25 in TPBS, pH 8.2, for 1 hour at RT. After rinses in TPBS and distilled water, the sections were stained with alcoholic uranyl acetate and lead citrate, rinsed again, air-dried, and viewed under the electron microscope. To evaluate the specificity of this antisera, sections were processed in the same way as described above, except that primary antisera were omitted or preadsorbed with the glutamate-glutaraldehyde-BSA conjugate. In both controls, glutamate-like immunoreactivity was completely abolished. To determine whether glutamate colocalizes with GABA, serial adjacent sections were processed for GABA immunocytochemistry (GABA antiserum was kindly provided by Dr. Somogyi) following the procedure as previously described (Hodgson et al., 1985; Somogyi and Soltesz, 1986; Nie and Wong-Riley, 1995).

Quantitative analysis at the EM level

Extensive EM quantitative analyses were performed on double-labeled samples of puffs and interpuffs from the three animals. All samples were treated identically to minimize technical variation. A two-dimensional measurement method, as described in our previous studies, was used in the present study for data collection and analysis (Wong-Riley et al., 1989a,b, 1994; Nie and Wong-Riley, 1995). Two assumptions were made with this approach: First, the distribution and orientation of all sampled elements within puffs and interpuffs were random; and second, the effects of fixation and tissue processing did not vary with region or with profile size.

Quantitative measurement of glutamate immunoreactivity To determine whether the differences in glutamate immunoreactivity in different tissue compartments were

statistically significant, we measured the surface density of gold particles over cellular profiles identified on the basis of their fine structural features. Random samples of the neuropil from puffs and interpuffs were analyzed in photographs taken at ×16,750. Generally, 8–10 nonoverlapping micrographs were taken from each puff or interpuff. Each micrograph sampled approximately 100 μm^2 of tissue comprising roughly 570 profiles. We have analyzed 120 such neuropil micrographs from puffs and 120 from interpuffs, totalling 12,000 μm^2 from each of the two regions. The neuropil profiles in which the density of gold particles was calculated were 1) axon terminals that contained presynaptic round vesicles and gave rise to asymmetric synapses—these were termed axon terminals forming asymmetric synapses or AA (Wong-Riley et al., 1989b); 2) axon terminals that contained flattened vesicles and made symmetric synapses—these were called axon terminals forming symmetric synapses or AS (Wong-Riley et al., 1989b); 3) randomly selected dendrites, including dendritic shafts and dendritic spines; and 4) glial processes usually containing glial filaments. Adjacent sections processed for GABA immunocytochemistry were used to determine the level of glutamate in GABAergic profiles. Cross-sectional areas of individual profiles were computed using a Calcomp 9000 digitizing tablet interfaced with an advanced digital microcomputer. Gold particles over different neuropil profiles, including those over mitochondria, were counted and expressed as the number of particles per μm^2 of each profile type. Aggregates of two or more gold particles were counted as one. To prevent overestimation of particle density, those over plasma membrane were not counted. For the analysis of cells, electron micrographs were prepared of all cells found in 18 samples from three animals (9 from puffs, 9 from interpuffs). Cells were classified as type A, B, or C neurons, or glial cells based on our previous criteria (Wong-Riley et al., 1989a, 1994). A total of 356 cells from puffs and 360 from interpuffs were analyzed following the same procedures described above.

Glutamate-IR axon terminals and synapses The numerical density, morphological feature, and postsynaptic targets of Glu-IR axon terminals and synapses in puffs and interpuffs were analyzed and compared: 1) Presynaptic axon terminals were considered Glu-IR if the density of Glu-IR gold particles over them was at least three times greater than that over nearby neuropil profiles. This quantitative criteria is based on studies using a similar approach in which the bouton to tissue gold particle density ratio is usually 2–5 times higher for glutamate-positive boutons than for other cellular compartments in several regions of the CNS (Somogyi et al., 1986; Ottersen, 1989a,b). Adjacent sections labeled for GABA were analyzed and compared to determine if Glu-IR and GABA-IR axon terminals were colocalized. As a result, we failed to find any axon terminal that was simultaneously immunoreactive for both Glu and GABA, but we did find a small proportion of asymmetric terminals that was not immunoreactive either for Glu or for GABA. The cross-sectional areas of glutamate-IR axon terminals from each region were digitized and computer-recorded. The mean size and numerical density of these terminals were also analyzed. 2) Glu-IR synapse was identified if it originated from a presynaptic axon terminal that was Glu-IR. Glu-IR, nonGlu-IR, and GABA-IR synapses were compared with two morphologically different types, symmetric and asymmetric ones (Colonnier, 1968). The mean lengths of glutamate-IR synapses in puffs and interpuffs were measured. The numerical densities of Glu-IR synapses and the ratio of Glu-IR to GABA-IR synapses in the neuropil of puffs and interpuffs were compared. 3) The postsynaptic neurons targeted by Glu-IR and/or GABA-IR synapses were identified as type A, type B (both are nonGABA-IR), and GABA-IR type C neurons (Wong-Riley et al., 1989a, 1994; Nie and Wong-Riley, 1995), and they were further classified into Glu-rich and Glu-poor neurons based on the criteria that Glu-IR gold particle density over Glu-rich neurons was at least two times higher than that over Glu-poor ones. The numerical density and ratio of Glu-IR and GABA-IR axosomatic synapses that each type of neurons received were analyzed. The postsynaptic dendritic elements targeted by Glu-IR synapses in the neuropil were classified as dendritic shafts and dendritic spines, as described above. These profiles were compared in puffs and interpuffs.

Mitochondria and CO activity Every detectable mitochondrion within each neuron and axon terminal from sampled regions of puffs and interpuffs was digitized and computer-recorded as to its area and degree of CO reactivity (dark, moderate, and light). As previously defined (Wong-Riley et al., 1989a,b), darkly reactive mitochondria possessed reaction product covering more than 50% of the outer surface of the inner mitochondria membrane and filling the intracristate space. Moderately reactive ones exhibited a moderate amount of reaction product that filled less than 50% of the inner mitochondrial membrane. Lightly reactive ones had little or no detectable reaction product. Based on the above criteria, areal density and CO activity of mitochondria in different profiles were compared between puffs and interpuffs.

Statistical analysis Parametric statistics (Student's t-test and analysis of variance) were used to analyze the numerical density and areal distribution of profiles. Nonparametric statistics (chi-square) were used for frequency analysis. Means were reported ± standard errors. A P value of 0.05 or less was considered significant.

RESULTS

Selective distribution of glutamate immunoreactivity

In sections from the neuropil of puffs and interpuffs doubly labeled by CO and glutamate, the distribution of Glu-IR gold particles was distinctly different over various profiles (Figs. 2–4). Presynaptic axonal terminals that had intense Glu-IR labeling were generally linked with asymmetric Gray's type I synaptic specializations (Figs. 2, 3A, 4). Small, clear, and round vesicles often clustered near the presynaptic membrane of the synaptic contact in this type of axon terminals. By contrast, sparse gold particles appeared randomly distributed over other profiles, including axon terminals forming symmetric synapses, glial processes, and many dendrites. Quantitative analysis (Table 1) indicated that the density of gold particles was significantly higher in presynaptic axon terminals that made asymmetric synapses (AA terminals) than those forming symmetric synapses (AS terminals), glial processes, and dendrites that were randomly examined ($P < 0.001$, in all cases). Dendrites contained significantly higher gold particle density than AS terminals ($P < 0.01$) and glial processes ($P < 0.001$).

In both puffs and interpuffs, 84% of terminals forming asymmetric synapses contained 3–10 times higher gold

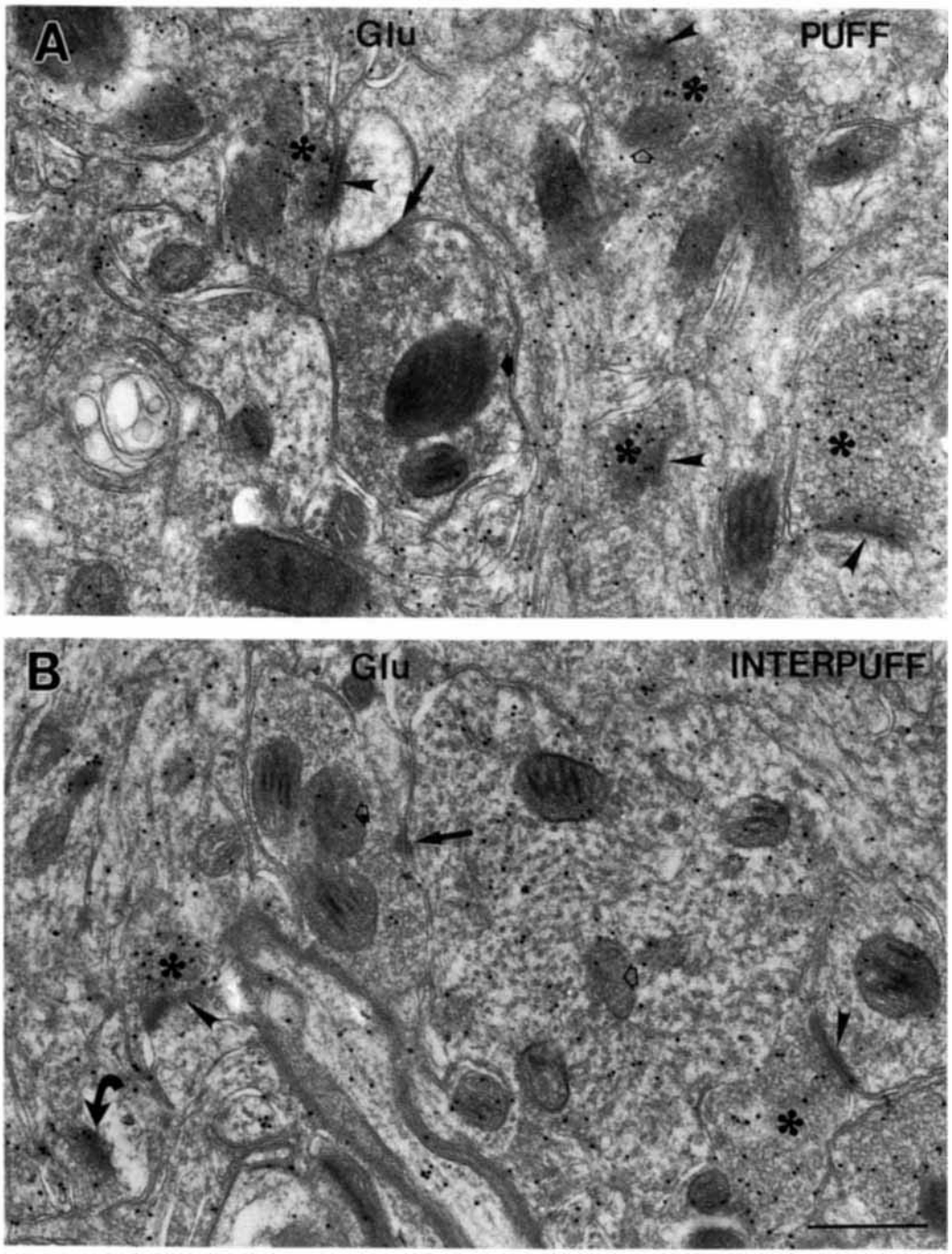

Fig. 2. Electron micrographs of the neuropil in a puff (**A**) and an interpuff (**B**) doubly labeled with CO and glutamate. Axon terminals with a high density of gold particles are identified as glutamate-immunoreactive (Glu-IR). The Glu-IR axon terminals (asterisks) in both puffs and interpuffs give rise to only asymmetric synapses (arrowheads) which target dendritic shafts or spines. The axon terminals forming symmetric synapses (arrows) contain very few gold particles, and are classified as nonGlu-IR symmetric axon terminals. These nonGlu-IR terminals linked to symmetric synapses usually contain more darkly and moderately CO-reactive mitochondria than Glu-IR ones. In our electron micrographs, dark, moderate and lightly CO-reactive mitochondria were indicated by shorter solid, half open, and open arrows, respectively. In B, the terminal forming an asymmetric synapse (curved arrow) shows only minimal immunostaining for glutamate and is classified as a nonGlu-IR asymmetric axon terminal. Scale Bar = 0.5 μm.

particle density than the other neuropil profiles. Based on the criteria described earlier, we identified them as Glu-IR presynaptic axon terminals (Figs. 2, 3A, 4). A small proportion (16%) of AA terminals, however, contained relatively low levels of glutamate that were only slightly higher than or close to those in the other nonGlu-IR profiles (Figs. 2,

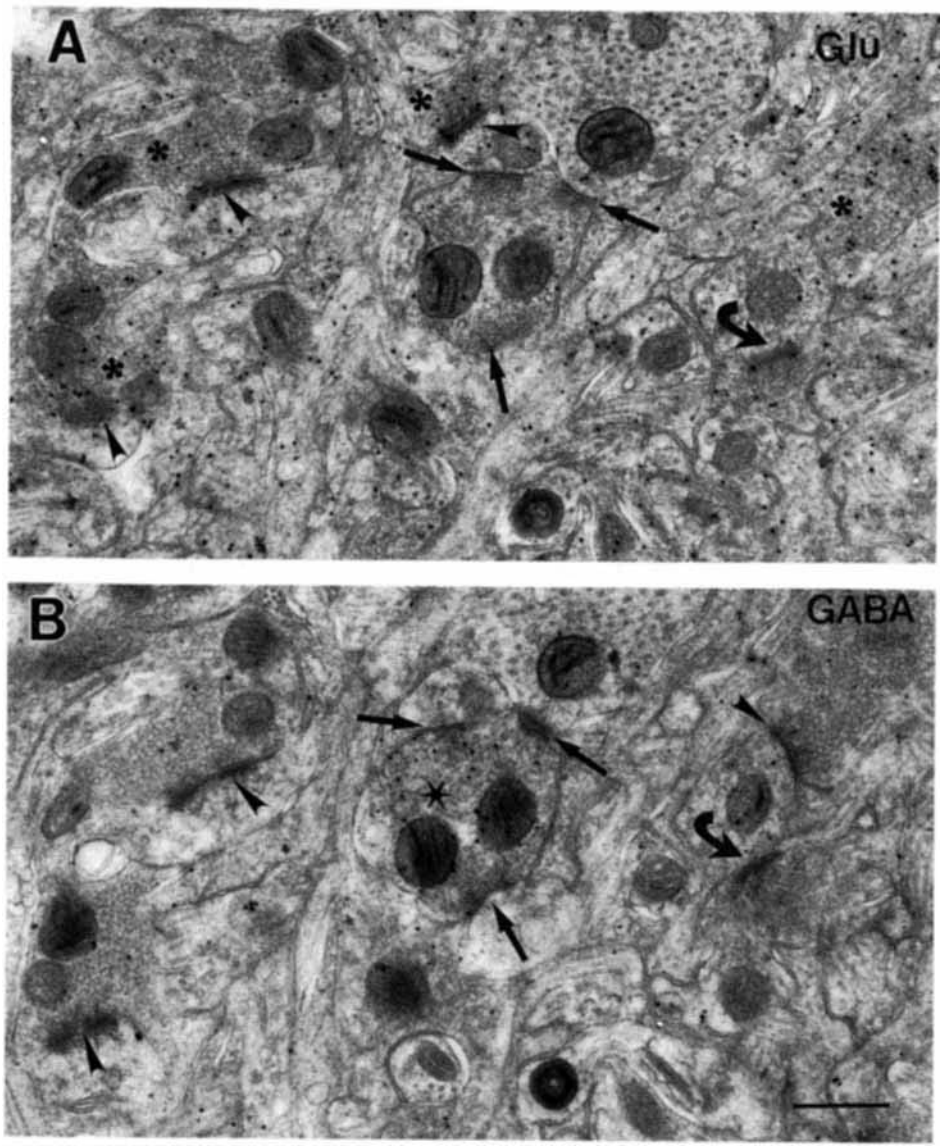

Fig. 3. Adjacent sections from a puff doubly labeled for CO and glutamate (**A**) or for CO and GABA (**B**). A: Glu-IR axon terminals (asterisks) give rise to asymmetric synapses (arrowheads). A nonGlu-IR axon terminal forms three symmetric synapses (arrows) and contains two darkly CO-reactive mitochondria. A small nonGlu-IR axon terminal also gives rise to an asymmetric synapse (curved arrow). B: The adjacent section immunostained for CO and GABA shows that: (1) all Glu-IR axon terminals (arrowheads) are nonGABA-IR; (2) a nonGlu-IR terminal forming an asymmetric synapse (curved arrow) is also non-GABA-IR; and (3) a nonGlu IR axon terminal (star) which forms three symmetric synapses (arrows) is intensely immunoreactive for GABA. Scale bar = 0.5 μm.

3A). Thus, we classified them as nonGlu-IR terminals forming asymmetric synapses. Serial sections alternately stained for either GABA or glutamate were examined to determine if axons with low levels of glutamate were GABA-IR, or if the two markers were colocalized in the same terminals (Figs. 3, 7–9). Results showed that presynaptic axon terminals can be divided into three major types: 1) axon terminals forming symmetric synapses that showed intense staining for glutamate but did not stain for GABA; 2) axon terminals forming asymmetric synapses with a moderate or low level of glutamate immunoreactivity but without staining for GABA; and 3) almost all axon terminals forming symmetric synapses, which only showed very low levels of staining for glutamate, were clearly GABA-immunoreactive (Figs. 3, 7–9). The lack of colocalization with GABA indicates that the distributions of glutamate and GABA in presynaptic axon terminals are completely separable. Thus, in the neuropil of both puffs and interpuffs, most of axon terminals forming asymmetric synapses were glutamate-immunoreactive, while nearly all of terminals forming symmetric synapses were GABAergic.

Glutamatergic axonal terminals and synapses in puffs versus interpuffs

As shown in a recent light microscopic study of the monkey visual cortex, immunoreactivity of glutamatergic terminals was particularly prominent in CO-rich puffs of

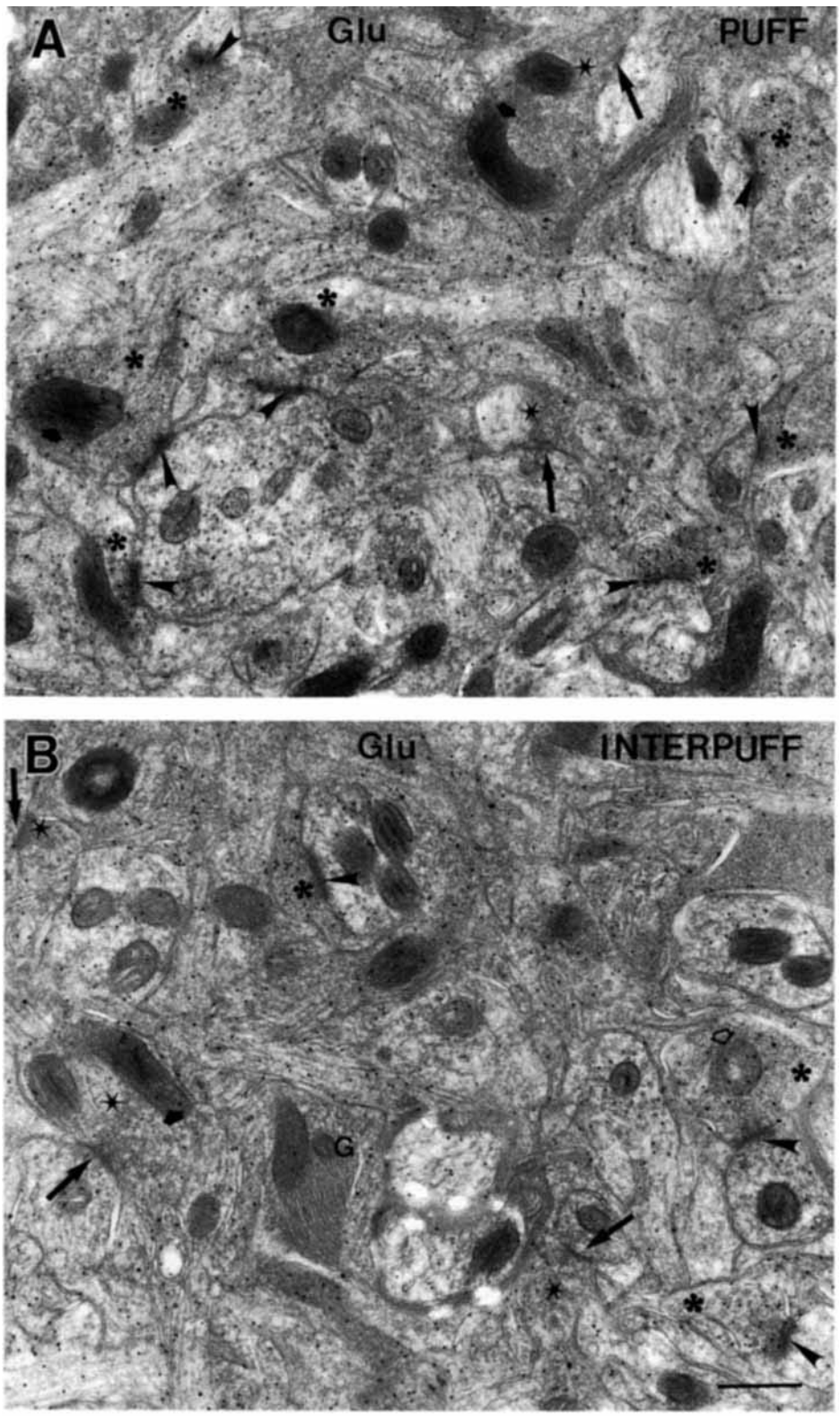

Fig. 4. Neuropil from a puff (**A**) and an interpuff (**B**) doubly labeled with CO and glutamate. In both regions, Glu-IR axon terminals (asterisks) give rise to asymmetric synapses (arrowheads), while symmetric synapses (arrows) originate from nonGlu-IR axon terminals (stars). The Glu-IR terminals (asterisks) in puffs contain more darkly and moderately CO-reactive mitochondria than those in interpuffs. Note also that there are only few gold particles on a glial process (G) in B. Scale bar = 0.5 μm.

TABLE 1. Comparisons of Glutamate Immunoreactivity in the Analyzed Neuropil Components Between Puffs and Interpuffs

Profile types	Mean gold particles per μm^2 ± SEM	Profiles N	Statistical comparisons		
Puffs					
AA terminals[1]	87.46 ± 3.41	1978	AA		
Dendrites	24.67 ± 2.34	836	<0.001	Den.	
AS terminals[2] (GABA-IR)	11.68 ± 0.53	1074	<0.001	<0.01	AS
Glial processes	4.28 ± 0.35	226	<0.001	<0.001	<0.01
Interpuffs					
AA terminals	83.85 ± 3.89	1651	AA		
Dendrites	26.63 ± 2.17	786	<0.001	Den.	
AS terminals (GABA-IR)	12.54 ± 0.69	974	<0.001	<0.01	AS
Glial processes	4.69 ± 0.15	217	<0.001	<0.001	<0.01

[1]Axon terminals that make asymmetric synapses.
[2]Axon terminals that make symmetric synapses.

TABLE 2. Comparisons of Glutamate-IR Axon Terminals Between the Neuropil of Puffs and Interpuffs[1]

	Puffs	Interpuffs	Statistical comparisons
Numerical density (N) per 100 μm^2 of neuropil	36.14 ± 2.2	23.33 ± 1.4	$P < 0.001$
Mean size (μm^2)	0.31 ± 0.04	0.24 ± 0.03	$P < 0.05$
Areal density (μm^2) per 100 μm^2 of neuropil	11.07 ± 0.43	5.71 ± 0.21	$P < 0.001$

[1]A total of 4,423 Glu-IR profiles from 12,000 μm^2 of neuropil in puffs and 2,774 profiles from an equivalent area of interpuffs were measured.

laminae II and III (Carder and Hendry, 1994). However, it would be difficult at the light microscopic level to determine if the difference in the staining pattern was caused by an increase in the numerical density and/or a greater mean size of Glu-IR terminals. To answer this question, the numerical density and cross-sectional areas of Glu-IR axon terminals in the neuropil from both puffs and interpuffs were measured and compared (Figs. 2–4). Table 2 shows that both the numerical density and mean size of Glu-IR axonal terminals were significantly greater in puffs than in interpuffs. Thus, both increased mean number and size of Glu-IR axonal terminals can contribute to their greater areal density in puffs.

Our results also showed that Glu-IR terminals in puffs appeared to contain more CO-reactive mitochondria than those in interpuffs (Figs. 2–4). To test whether the difference is significant, we measured the areal distribution and CO activity of mitochondria in these terminals between the two regions. Quantitative analysis (Fig. 5) indicated that the areal density of mitochondria in Glu-IR axon terminals in puffs were greater than that in interpuffs ($P < 0.01$). Moreover, Glu-IR terminals in puffs contained three times more darkly CO-reactive mitochondria than those in interpuffs ($P < 0.001$). To compare with those in GABAergic terminals, parallel measurements were carried out in GABA-IR terminals. Figure 5 shows that GABA-IR terminals in each region contained significantly more darkly CO-reactive mitochondria than glutamate-IR ones ($P < 0.001$).

To determine the characteristics of glutamate-IR synapses in the neuropil of puffs and interpuffs, a total of 4,732 synapses from puffs and 3184 from interpuffs were analyzed. In both regions, all glutamate-IR synapses were asymmetric ones (Figs. 2–4). However, about 16% of asymmetric synapses originated from presynaptic terminals that were not intensely immunostained by glutamate (Figs. 2, 3). No synapse with symmetric features was found to be glutamate-immunoreactive, while almost all symmetric synapses were GABA-IR in the two regions (Figs. 3, 7, 9). Quantitative analysis showed that there was a higher numerical density of glutamate-IR synapses in puffs than in interpuffs ($P < 0.001$, Table 3). Table 3 also indicates that the ratio of Glu-IR to GABA-IR synapses in puffs was significantly higher than that in interpuffs ($P < 0.01$). However, the mean lengths of glutamate-IR synapses were not significantly different between the two regions: 0.23 ± 0.04 μm in puffs versus 0.23 ± 0.05 in interpuffs ($P > 0.05$). To determine whether these synapses preferentially targeted different neuropil elements in the two regions, postsynaptic targets of Glu-IR synapses were also compared. In both regions, about 72% of glutamate-IR synapses targeted dendritic spines, 28% of them contacted dendritic shafts.

Neurons: somatic innervation and CO levels

To determine if CO levels in postsynaptic neurons were correlated with the type and proportion of axosomatic synapses they received and if these neurons contained different levels of glutamate, a total of 334 neurons from puffs and 336 from interpuffs were analyzed. Classification of neurons into type A, type B (both are nonGABA-IR), and GABA-IR type C neurons was based on criteria previously described (Wong-Riley et al., 1989a, 1994; Nie and Wong-Riley, 1995), and they were further identified as Glu-rich or Glu-poor neurons based on their glutamate levels.

Glu-rich, type A, neurons (Fig. 6) This type of neurons was relatively small but abundant, which comprised about 59% of the neuronal population (Wong-Riley et al., 1989a, 1994). Their thin rim of cytoplasm contained only a few organelles, including a small number of mitochondria, most of which were only lightly reactive for CO in both puffs and interpuffs (Figs. 6, 11). They were strongly immunoreactive for glutamate (Figs. 6, 7a; Table 4), but consistently not immunoreactive for GABA (Fig. 7d). Moreover, these Glu-rich type A neurons received exclusively symmetric, nonGlu-IR, axosomatic synapses (Figs. 6, 7a). Adjacent sections stained by GABA antibodies confirmed that these non-Glu-IR synapses (Fig. 7a) were GABA-immunoreactive (Fig. 7d), consistent with our previous findings (Nie and Wong-Riley, 1995). Thus, type A neurons in both puffs and interpuffs possessed the following major characteristics: 1) small size with varying shapes, probably including both small pyramidal and nonpyramidal neurons; 2) immunocytochemically rich in glutamate but lacked GABA in their cytoplasm; 3) contained relatively few mitochondria, nearly all with very low levels of CO activity; and 4) received only GABA-IR axosomatic synapses.

Glu-rich, type B, neurons (Fig. 6) These were medium and large pyramidal neurons in puffs and interpuffs (Wong-Riley et al., 1989a, 1994). They contained a wealth of organelles, and their mitochondria were more densely packed than those in type A cells. Mitochondria in these neurons were mainly lightly and moderately reactive for CO in both regions (Figs. 6, 11). They contained a high level of glutamate, but lacked GABA immunoreactivity in their cytoplasm (Figs. 6, 7; Table 4). Like type A cells, they also received only GABA-IR synapses on their somata (Fig. 7e,f). Thus, type B cells were large, pyramidal, glutamate-rich neurons, which received only inhibitory GABA-IR axosomatic synapses and contained mainly low to moderate levels of CO activity.

GABA-IR, but Glu-poor, type C neurons (Figs. 8, 9) They were the medium-sized, highly CO-reactive nonpyramidal neurons (Wong-Riley et al., 1989a, 1994). Neuro-

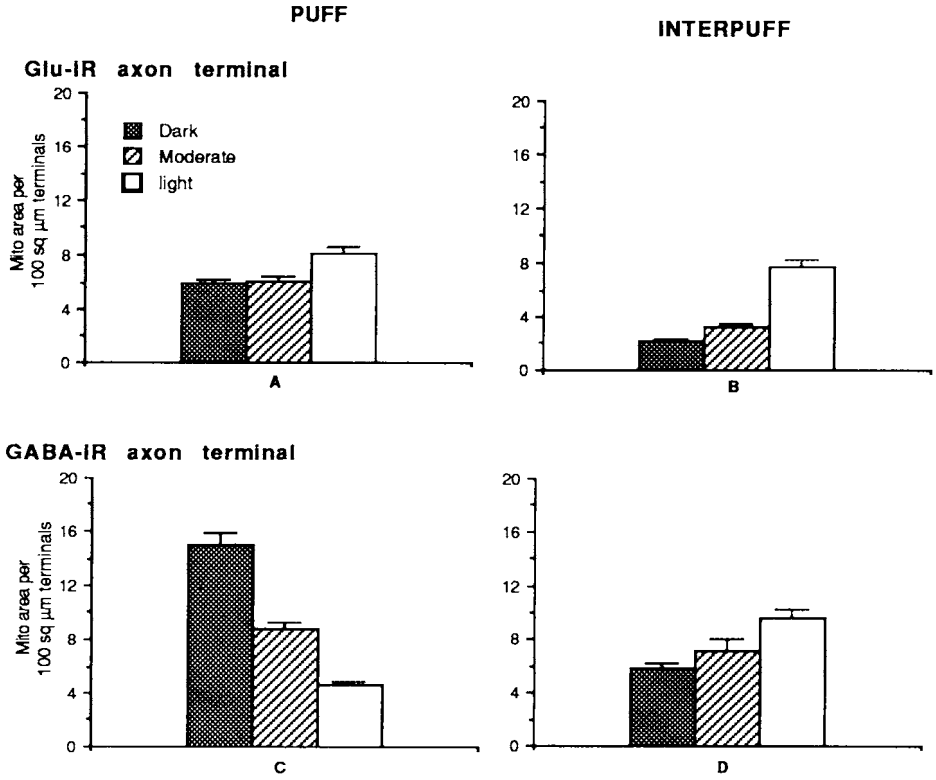

Fig. 5. Areal distribution of mitochondria in Glu-IR and GABA-IR axon terminals per 100 μm^2 of terminal area. Data are presented as mean values ± S.E.M. The Glu-IR axon terminals in puffs (**A**) contain three times more darkly CO-reactive mitochondria than those in interpuffs (**B**) ($P < 0.001$). The GABA-IR axon terminals (**C** and **D**) in both regions contain a greater proportion of darkly CO-reactive mitochondria than Glu-IR terminals (A and B) (P 0.001).

TABLE 3. Comparisons of Glu-IR, GABA-IR, and Non-Glu-IR/Non-GABA-IR Synapses in the Neuropil of Puffs and Interpuffs[1]

Synapses per 100 μm^2 neuropil	Puffs		Interpuffs		Statistical comparisons
	AA[2]	AS[3]	AA	AS	
Glu-IR	24.27 ± 1.32	—	15.13 ± 0.84	—	$P < 0.001$
GABA-IR	—	10.11 ± 0.72	—	8.32 ± 0.51	$P < 0.05$
non-Glu-IR	4.62 ± 0.25	—	2.72 ± 0.16	—	$P < 0.001$
non-GABA-IR	—	0.40 ± 0.02	—	0.33 ± 0.14	$P < 0.05$
Ratio of Glu-GABA-IR	2.41 ± 0.11		1.81 ± 0.08		$P < 0.01$

[1]Total count of synapses: 4,732 from puffs and 3,184 from interpuffs.
[2]Synapses from asymmetric axon terminals.
[3]Synapses from symmetric axon terminals.

chemically, these cells were clearly immunoreactive for GABA (Figs. 8, 9), confirming our previous findings (Nie and Wong-Riley, 1995). However, these GABA-IR type C neurons contained a level of glutamate that was 50% lower than those in Glu-rich type A and type B neurons (Figs. 8, 9; Table 4). Their cytoplasm was richly supplied with organelles, including several perinuclear Golgi complexes, rough endoplasmic reticulum in thin strands and short stacks, free ribosomes, microtubules, and neurofilaments. In both puffs (Fig. 8) and interpuffs (Fig. 9), they contained abundant mitochondria that were mainly darkly and moderately reactive for CO. Moreover, these GABA-IR type C neurons received both Glu-IR and GABA-IR synapses on their cell bodies (Figs, 8–9). Quantitative analysis (Fig. 11) indicated that this type of neurons contained three times more darkly CO-reactive mitochondria than Glu-rich type A or type B neurons, which received only GABA-IR synapses in both regions ($P < 0.001$). Our results also showed that GABA-IR type C neurons in puffs possessed more darkly CO-reactive mitochondria than those in interpuffs ($P < 0.001$, Fig. 11). In puffs, this type of neurons received significantly more Glu-IR synapses on their somata than those in interpuffs: 10.54 ± 0.32 versus 6.21 ± 0.28 per 100 µm perikaryal perimeter in puffs and interpuffs, respectively ($P < 0.001$). In addition, the ratio of Glu-IR to GABA-IR axosomatic synapses targeting GABAergic neurons in puffs was also significantly higher than that in interpuffs (2.06 ± 0.05 vs. 1.35 ± 0.04, $P < 0.01$).

In order to determine whether the levels of glutamate were different between neurons and glial cells, we measured the density of gold particles immunostained by glutamate over the cytoplasm of glial cells. Quantitative analysis indicated that glial cells consistently contained a much lower level of glutamate than neurons (Fig. 10; Table 4).

DISCUSSION

By combining CO histochemistry and postembedding glutamate immunocytochemistry on the *same* ultrathin sections, we have tested the hypothesis that the capacity for oxidative metabolism in postsynaptic neurons and neuropil of puffs and interpuffs is positively correlated with the proportion of excitatory Glu-IR synapses they receive. The

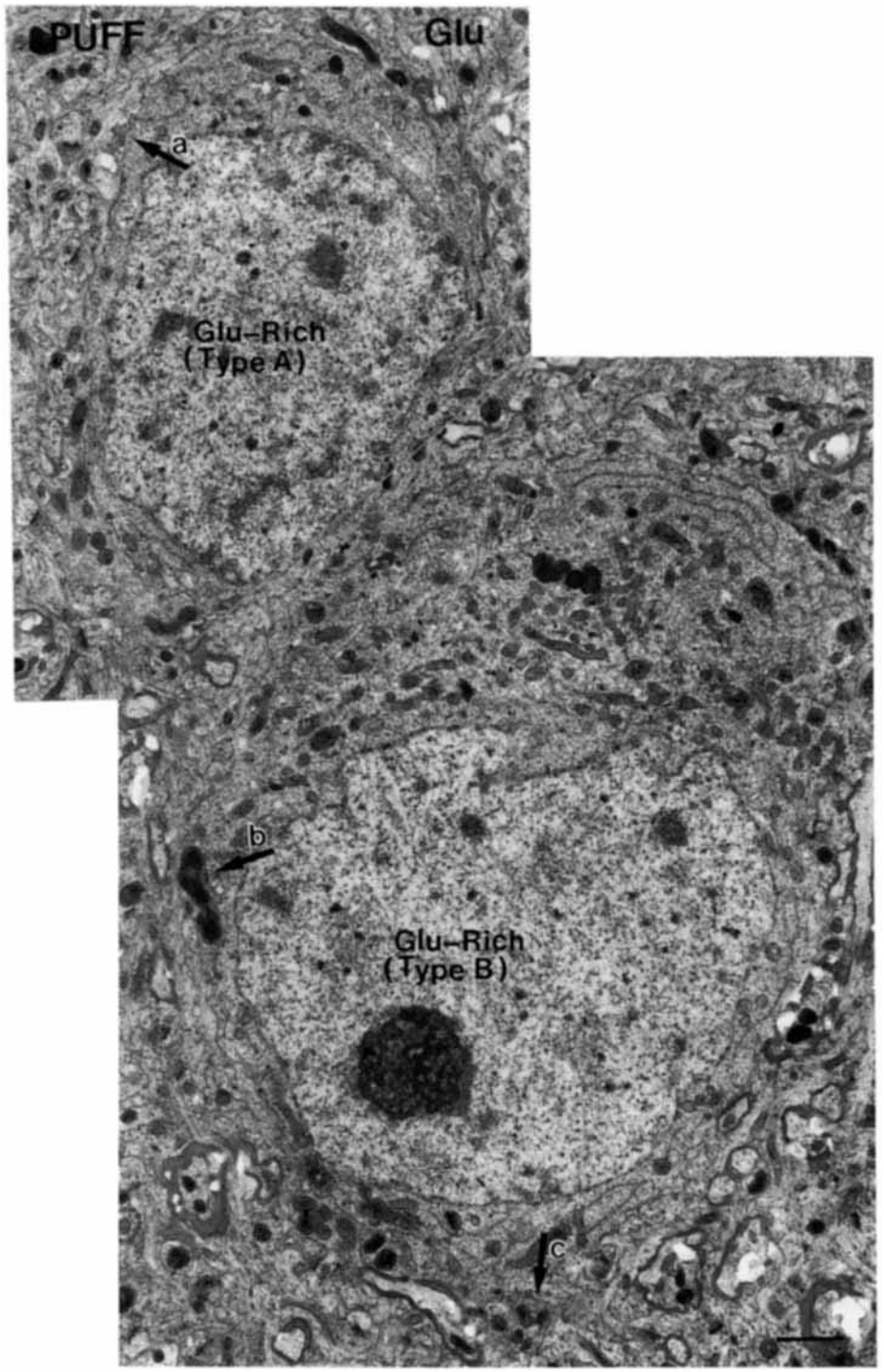

Fig. 6. An electron micrograph of two Glu-rich neurons from a puff doubly labeled with CO and glutamate. The two neurons have a much higher density of immunogold labeling than the nearby neuropil. The upper neuron has the features of small, type A cells described previously (Wong-Riley et al., 1989a). Its thin rim of cytoplasm contains very few organelles, including mitochondria that are mostly lightly reactive for CO. The lower neuron is consistent with type B pyramidal cells as classified previously (Wong-Riley et al., 1989a). It contains mainly lightly and some moderately CO-reactive mitochondria. The two types of neurons receive exclusively nonGlu-IR symmetric synapses on their cell bodies (arrows). The three axosomatic synapses (a–c) contacting the two neurons are magnified in Figure 7. Scale bar = 1 μm.

following findings support our hypothesis: 1) Most presumed excitatory axon terminals (84% of asymmetric ones) in both puffs and interpuffs were intensely immunoreactive for glutamate, indicating that glutamate might be used as their major excitatory neurotransmitter. 2) GABA-IR neurons received mainly Glu-IR axosomatic synapses and had a

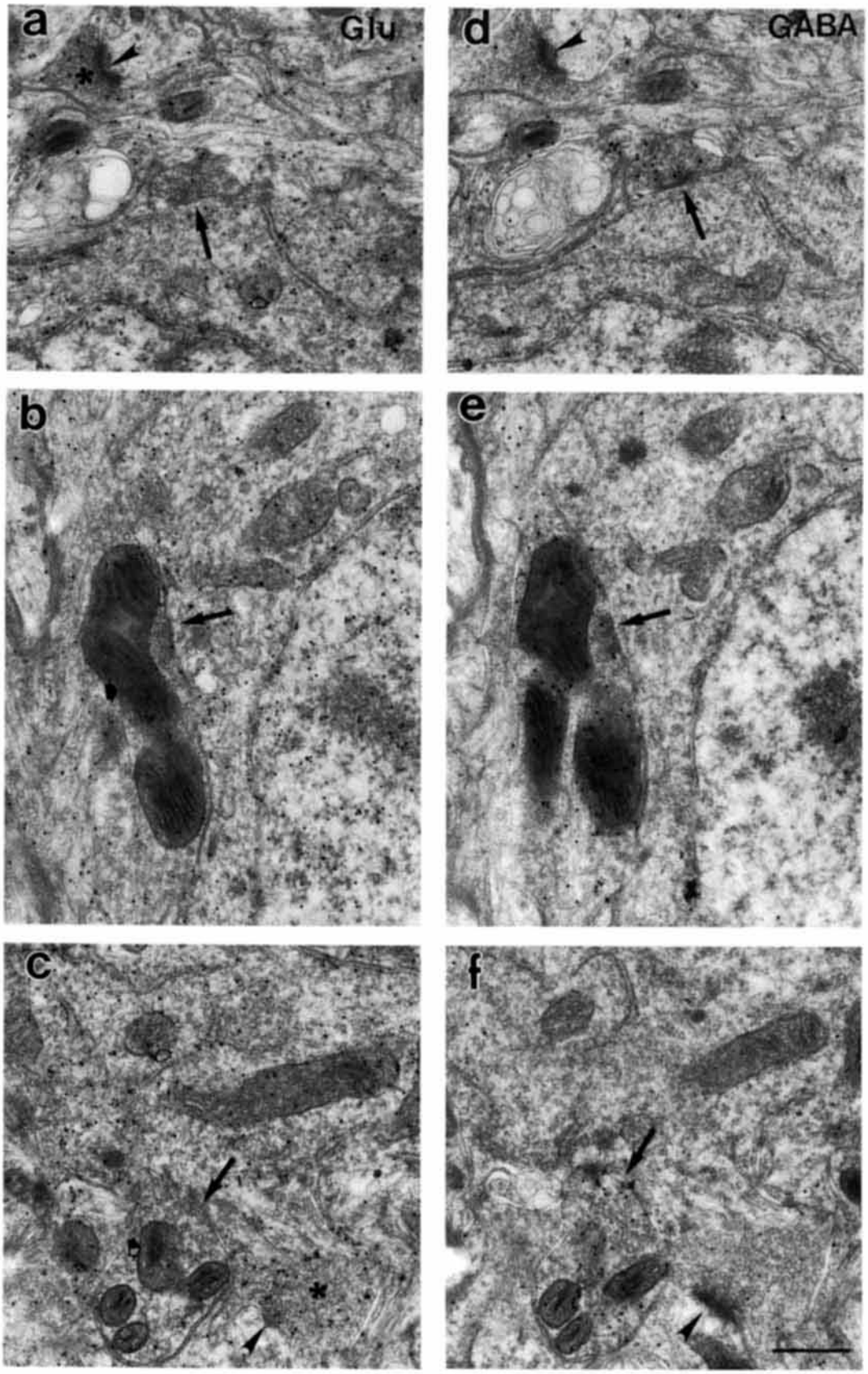

Fig. 7. A higher magnification of three axosomatic synapses (a–c in Fig. 6) contacting the two Glu-rich neurons. Adjacent sections were doubly labeled with CO and glutamate (**a–c**), or with CO and GABA (**d–f**). In Glu-stained sections (a–c), there is a higher density of gold particles in the cytoplasm of the two neurons than the nearby neuropil. The two Glu-rich neurons contain mainly lightly CO-reactive mitochondria. Note that the three axosomatic synapses (arrows) that Glu-rich neurons receive are symmetric synapses and originate from nonGlu-IR axon terminals, which contain mainly darkly and moderately CO-reactive mitochondria. Adjacent GABA-reacted sections (d–f) show that these three nonGlu-IR terminals are intensely immunoreactive for GABA, while the cytoplasm of the two neurons is not immunoreactive for GABA. Note also that the two Glu-IR axon terminals in the neuropil of a and c (asterisks) give rise to asymmetric synapses (arrowheads), and adjacent sections (d and f) show that they are nonGABA-IR. Scale bar = 0.5 μm.

TABLE 4. Comparisons of Glutamate Immunoreactivity in the Analyzed Cells Between Puffs and Interpuffs

Cell types	Mean gold particles per μm^2 ± SEM	Cells N[1]	Statistical comparisons		
Puffs					
Type A	44.61 ± 2.96	194	Type A		
Type B	47.74 ± 2.79	58	NS	Type B	
Type C (GABA-IR)	18.16 ± 1.06	82	<0.001	<0.001	Type C
Glial	6.53 ± 0.41	22	<0.001	<0.001	<0.001
Interpuffs					
Type A	43.12 ± 2.46	189	Type A		
Type B	46.38 ± 2.10	62	NS	Type B	
Type C (GABA-IR)	17.64 ± 1.27	85	<0.001	<0.001	Type C
Glial	5.47 ± 0.38	24	<0.001	<0.001	<0.001

[1]For each cell analyzed, 10 randomly selected cytoplasmic regions, each with 1 μm^2 of area, were used to measure the density of gold particles.

higher level of CO activity than Glu-rich (nonGABA-IR) neurons, which received only inhibitory GABA-IR synapses on their cell bodies. 3) CO-rich puffs received more Glu-IR synapses and a higher ratio of Glu- to GABA-IR synapses than CO-poor interpuffs. Moreover, Glu-IR axon terminals in puffs contained three times as many CO-reactive mitochondria than those in interpuffs, suggesting that the former may be functionally more active.

Glutamate as a major synaptic transmitter in puffs and interpuffs

With double labeling of CO and glutamate at the EM level, both the ultrastructure and CO activity of brain samples were well preserved. Thus, it enabled us to compare morphological features and metabolic differences in the tissue with confidence. Moreover, postembedding glutamate immunocytochemistry provided a necessary and optimal means for quantifying the subcellular distribution of glutamate immunoreactivity and for identifying Glu-IR presynaptic axon terminals (Somogyi et al., 1986; Storm-Mathisen and Ottersen, 1988; Ottersen, 1989a,b). It has been reported that the number of immunogold particles per unit area derived from the sections containing osmium-treated glutamate conjugates was proportional to the concentration of fixed glutamate (Ottersen, 1989b). The specificity of this antibody in the present study was verified by the complete abolishment of immunoreactivity by preadsorption with glutamate. Thus, the relative level of glutamate immunoreactivity represents the relative amount of glutamate in various profiles. Since glutamate is an amino acid that acts at two major, well-recognized levels in neuronal functions: neurotransmitter pool and metabolic pool (Fonnum, 1984; Erecinska and Silver, 1990), one of the most important issues to be addressed is the presence of glutamate in all cells, where it is necessary for cellular metabolism. Indeed, glutamate is metabolically involved in protein synthesis as an amino acid, in citric acid cycle as an intermediate metabolite, and in GABA synthesis as its precursor (Fonnum, 1984; Erecinska and Silver, 1990).

One of the criteria for a neurochemical to be a functional neurotransmitter is its highly selective distribution in certain presynaptic axon terminals (Fonnum, 1984; Somogyi et al., 1986; Tsumoto, 1990). The present study indicates that there is a significantly higher content of glutamate in axon terminals forming asymmetric synapses than in GABAergic terminals, dendrites, and glial processes, consistent with previous studies (Somogyi et al., 1986; Montero and Wenthold, 1989; Ottersen, 1989a,b; Montero, 1990; van den Pol et al., 1990). Our interpretation, on the one hand, is that a low level of glutamate with relatively uniform distribution in all cellular profiles represents its various metabolic functions (Hertz, 1979; Erecinska and Silver, 1990). However, a much lower level of glutamate in GABAergic terminals and glial processes, as compared to those in the other profiles, might result from a rapid conversion of glutamate to GABA by the action of glutamate decarboxylase in GABAergic terminals, and of glutamate to glutamine via glutamine synthetase in glial cells (Erecinska and Silver, 1990). In fact, nearly all axon terminals forming symmetric synapses with low glutamate levels in both puffs and interpuffs are GABAergic, suggesting that glutamate exists there mainly as an intermediate metabolite rather than as a neurotransmitter (Nie and Wong-Riley, 1995; the present study). On the other hand, the higher level of glutamate in axon terminals forming asymmetric synapses may represent the neurotransmitter pool there (Somogyi et al., 1986; Tsumoto, 1990). Several lines of evidence support this interpretation: First, the terminals intensely labeled by glutamate have morphological features (such as round vesicles and asymmetric synapses) generally associated with excitatory neurotransmission (Gray, 1959; Uchizono, 1965; Somogyi et al., 1986; van den Pol et al., 1990; Broman and Ottersen, 1992). In addition, there is a strong correlation between the density of glutamate immunogold particles and that of synaptic vesicles in asymmetric axon terminals, but not in symmetric GABAergic ones (Kharazia and Weinberg, 1994; Broman and Ottersen, 1992). Second, the high level of glutamate in these axons is not primarily due to its role in general metabolism (Cotman et al., 1987; Ottersen et al., 1990; Osen et al., 1995). After depleting the metabolic pool of glutamate from neuronal cell bodies, these axon terminals still showed a robust immunoreactivity for glutamate. However, stimuli such as high potassium or veratridine in the presence of calcium, which depolarized neurons and induced the release of neurotransmitter, did cause a loss of axonal glutamate immunoreactivity (Cotman et al., 1987; Ottersen et al., 1990; Osen et al., 1995). Third, antagonists for glutamate receptors can powerfully block the excitatory actions mediated by glutamate in the visual cortex, indicating that glutamate is involved in excitatory synaptic transmission in this region (Foster and Fagg, 1984; Tsumoto, 1990; Moriyoshi et al., 1991). Together with the present results, it is likely that most axon terminals forming asymmetric synapses use glutamate as their major neurotransmitter in both puffs and interpuffs. However, since a small proportion (about 16%) of asymmetric axon terminals contained only moderate or low levels of glutamate, we cannot rule out the possibility that the amount of glutamate as transmitter in these terminals may be below the level of our detection, or that these terminals may use other neurotransmitters, such as aspartate (Hicks, 1987; Ottersen, 1989a; Conti, 1991).

Within puffs and interpuffs, the perikaryal labeling for glutamate in nonGABAergic type A and type B neurons was two times greater than that in GABAergic ones. Our results are generally in agreement with previous studies that pyramidal and some nonpyramidal neurons, which are consistent with our type B and type A neurons, respectively, were enriched in glutamate in their somata, suggesting that these neurons may chemically belong to an excitatory neuronal population, and give rise to glutamatergic terminals (Conti et al., 1988, 1989; Wong-Riley et al., 1989a, 1994; Carder and Hendry, 1994; Nie and Wong-Riley,

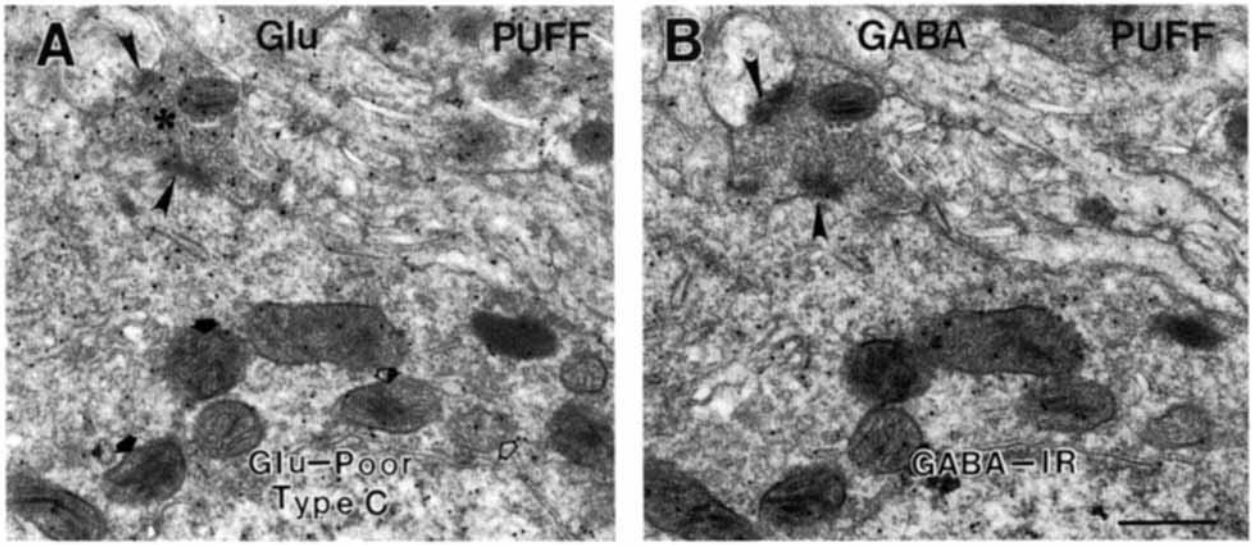

Fig. 8. Electron micrographs of two adjacent sections showing the same Glu-poor neuron from a puff that was doubly labeled by CO and glutamate (**A**), or by CO and GABA (**B**). A: This neuron is poorly immunostained by glutamate, and it receives an asymmetric synapse (arrowhead) originating from an axon terminal (asterisk) which is strongly immunoreactive for glutamate. The cytoplasm of the neuron contains mainly darkly and moderately CO-reactive mitochondria. B: Adjacent section shows that this neuron is GABA-immunoreactive, while the Glu-IR axon terminal contacting it is not immunoreactive for GABA. Scale bar = 0.5 μm.

1995). However, it may be argued that the somatic labeling does not necessarily reflect a transmitter pool of glutamate, since a considerable portion of glutamate is estimated to be involved in protein synthesis and other metabolic functions in the perikarya (Somogyi et al., 1986; Erecinska and Silver, 1990; Ottersen et al., 1990). A recent study has demonstrated that the granule cell bodies intensely labeled for glutamate in the slice preparation of pig brain failed to display the depolarization-induced decrease in glutamate immunolabeling typical of the parallel fiber terminals (Osen et al., 1995). This suggests that the perikarya of these Glu-rich cells may contain a sizable pool of glutamate for metabolic needs, and has no direct access to synaptic release mechanisms.

Presynaptic contacts and oxidative capacity in postsynaptic neurons

One of the striking findings that emerged from our study is that there is a consistent correlation between the neurochemical types and frequency of *presynaptic* contacts and the level of oxidative metabolism as revealed by CO activity in *postsynaptic* neurons. GABAergic neurons receive mainly excitatory Glu-IR axosomatic synapses, and they contain primarily darkly CO-reactive mitochondria. Direct depolarization of somatic membrane by excitatory synapses would place a greater energy demand on the perikarya for ATP-dependent membrane repolarization than would hyperpolarization (Ruscak and Whittam, 1967; Lowry, 1975; Duckrow et al., 1981; Wong-Riley, 1989, 1994). Their rich supply of darkly CO-reactive mitochondria is consistent with our hypothesis that these neurons do need a greater oxidative capacity for elevated levels of spontaneous and/or synaptically evoked activity, mainly mediated by Glu-IR synapses. This is further reinforced by our present findings that GABA-IR neurons in puffs receive a greater proportion of Glu-IR axosomatic synapses and contain more darkly CO-reactive mitochondria than those in interpuffs. Thus, the increased energy demands, as a result of strong synaptic innervation by glutamate, in these postsynaptic neurons could accelerate the rate of energy syntheses through up-regulating the activity/content of energy-generating enzymes, such as CO. The regulation of CO levels in response to changes in energy demand due to presynaptic activity is likely to involve two different mechanisms: short-term and long-term regulation (Erecinska and Silver, 1989; Wong-Riley, 1994). Short-term regulation of functional activity could be affected by allosteric alterations via local changes in the ratio of ADP/ATP, pH values, and other metabolites (Erecinska and Silver, 1989). The greater consumption of energy subsequent to excitatory depolarization leads to a local increase in ADP/ATP ratio. Increased ADP could signal mitochondria to cease movement, resulting in clustering of mitochondria in regions of high ATP demand (Bereiter-Hahn and Voth, 1983). In addition, the inhibition of CO activity due to the binding of ATP, as an allosteric factor, could be relieved following an increased ratio of ADP/ATP (Erecinska and Silver, 1989). On the other hand, long-term regulation of CO activity could occur at the transcriptional and translational levels by affecting the number of functional enzyme molecules (Hevner and Wong-Riley, 1990, 1993). Chronic depolarizing stimulation, such as electrical excitation of muscles in rats, led to an increased expression of mRNAs for CO accompanied by an elevated level of CO activity (Williams et al., 1987; Hood, 1990). Physiological studies have shown that excitatory postsynaptic potentials induced by electrical stimulation of axons can be predominantly blocked by the addition of glutamate receptor blockers, such as kynurenic and CNQX, suggesting the involvement of glutamate-mediated excitation (Hicks, 1987; Tsumoto, 1990; Wuarin and Dudek, 1991). Likewise, monocular deprivation of excitatory afferent impulses dramatically reduces CO activity in the monkey striate cortex by down-regulating the expression of CO mRNAs and proteins, particularly in GABAergic neurons

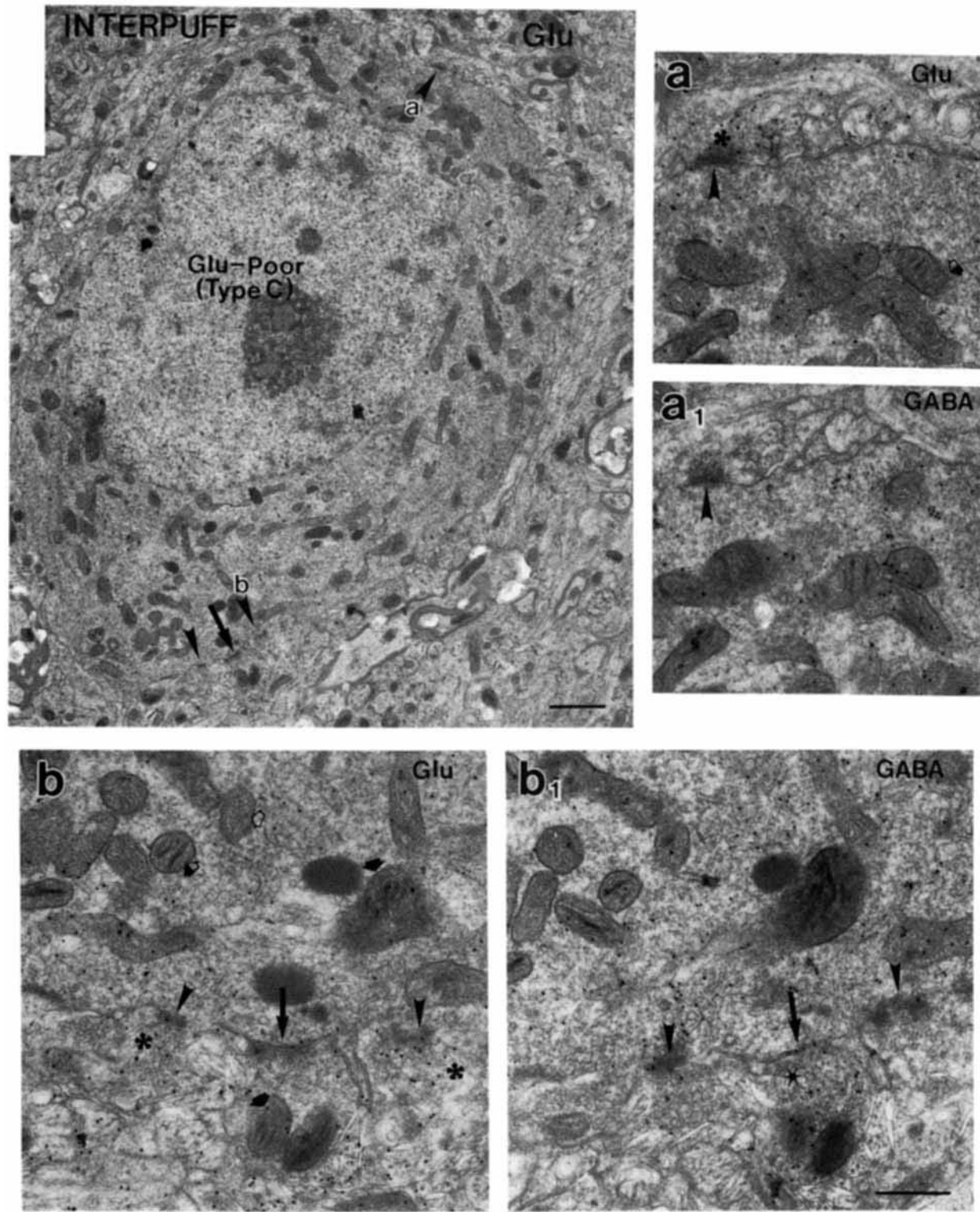

Fig. 9. A Glu-poor neuron from an interpuff. This neuron is only lightly immunoreactive for glutamate. Its cytoplasm contains many mitochondria that are mainly moderately reactive for CO. This neuron receives Glu-IR (arrowheads) and nonGlu-IR synapse (arrow) on its cell body. **Insets a and b:** Higher magnifications of axosomatic synapses which target this neuron. In inset a, this neuron is lightly immunoreactive for glutamate, and receives an asymmetric axosomatic synapse (arrowhead) from a Glu-IR axon terminal (asterisk). The adjacent section ($\mathbf{a}_1$) which was doubly labeled by CO and GABA shows that this neuron is GABA-immunoreactive, while the Glu-IR asymmetric axon terminal is not immunoreactive for GABA. In inset b, two asymmetric synapses (arrowheads) from Glu-IR axon terminals (asterisks) and one symmetric synapse (arrow) from nonGlu-IR axon terminal target this neuron. The adjacent section ($\mathbf{b}_1$) doubly labeled by CO and GABA shows that the two Glu-IR axon terminals are not immunoreactive for GABA (arrowheads), while the nonGlu-IR axon terminal which forms a symmetric synapse (arrow) is GABA-immunoreactive. Note that its cytoplasm contains mitochondria with different CO-reactive levels, including darkly, moderately, and lightly reactive ones. Scale bars = 1 μm in the neuron and 0.5 μm in insets.

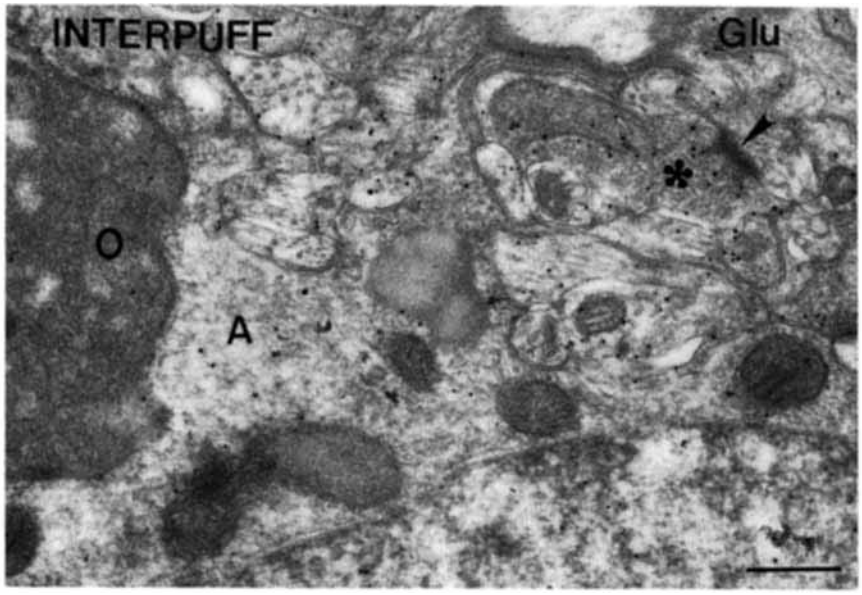

Fig. 10. Glial cells (O: oligodendrocyte; A: astrocyte) doubly labeled by CO and glutamate. These two glial cells show very few immuno-gold particles and very low levels of CO. An axon terminal (asterisk) in the nearby neuropil which forms an asymmetric synapse (arrowhead) is intensely immunoreactive for glutamate. Scale Bar = 0.5 μm.

(Hendry and Jones, 1986; Hevner and Wong-Riley, 1990, 1993; Nie et al., 1995). Thus, the present findings suggest that CO-rich, GABAergic neurons do require a sustained excitatory input, mediated mainly by glutamatergic synapses, to maintain their heightened levels of oxidative metabolism.

In contrast, Glu-rich type A and B neurons that contain mainly lightly CO-reactive mitochondria receive exclusively inhibitory GABA-IR synapses on their somata, where they are generally thought to be much more efficacious in inhibition than those farther away on distal dendrites (Rall et al., 1967; Shepherd, 1979; Somogyi, 1989). Physiologically, GABA-mediated synaptic transmission leads to hyperpolarization of postsynaptic neurons, and thus reduces the response in these cells to excitatory signals from their dendrites (Somogyi, 1989; Berman et al., 1991, 1992). Neurons are much less excitable if they are under greater inhibition (Somogyi, 1989) and, metabolically, repolarization subsequent to hyperpolarization mediated by GABA synapses is mainly passive, and requires little energy (Ruscak and Whittam, 1967; Duckrow et al., 1981; Wong-Riley, 1989, 1994). Thus, neurons under chronic GABA inhibition are expected to have low metabolic activity, in agreement with our present findings.

Our results also indicate that the level of oxidative metabolism in neurons does not bear a direct relationship with their glutamate levels. Glu-rich neurons and axon terminals contain much lower CO levels than GABAergic ones, which are poor in glutamate. Thus, the level of oxidative metabolism in postsynaptic neurons is not correlated with the type of transmitter they contain, but rather, are closely dependent upon the type and intensity of innervation they receive. On the other hand, local glutamate levels in neuronal compartments, especially serving as neurotransmitters, may rely mainly on the presence of specific mechanisms for its synthetic machinery and/or reuptake pathway (Hertz, 1979; Fonnum, 1984; Tsumoto, 1990; Conti, 1991).

Excitatory axon terminals and synapses in puffs versus interpuffs

Our present study demonstrates for the first time that puffs receive significantly more Glu-IR synapses and a greater proportion of Glu- to GABA-IR synapses than interpuffs. This is consistent with a more intense immunoreactivity for glutamate, mainly in presumed labeled axon terminals, in puffs than in interpuffs shown at the light microscopic level (Carder and Hendry, 1994). Our results also indicate that glutamatergic axon terminals contain three times more darkly CO-reactive mitochondria and have a larger mean size in puffs than those in interpuffs, suggesting that the former may be synaptically more active. Although the functional significance of terminal size remains unclear, large terminals are associated with strong synaptic drive (Pierce and Lewin, 1994). Metabolically, the synthesis, synaptic release, and reuptake of glutamate have a stringent requirement for ATP that can only be fully satisfied by oxidative metabolism in the CNS (Natio and Ueda, 1983, 1985; Nicholls, 1989). Moreover, most of the energy cost in the brain can be attributed to active ion transport not only at postsynaptic but also at presynaptic sites, presumably to restore the ionic gradients across the neural membranes subsequent to presynaptic electrical activity (Ruscak and Whittam, 1967; Lowry, 1975). Studies in insects, crustaceans, and lampreys have shown that the firing pattern of presynaptic terminals is closely correlated with the number and size of mitochondria there (Atwood and Wojtowicz, 1986; Shupliakov et al., 1992). Tonically active synapses contain a large amount of mitochondrial material and tend to have a heightened firing rate as

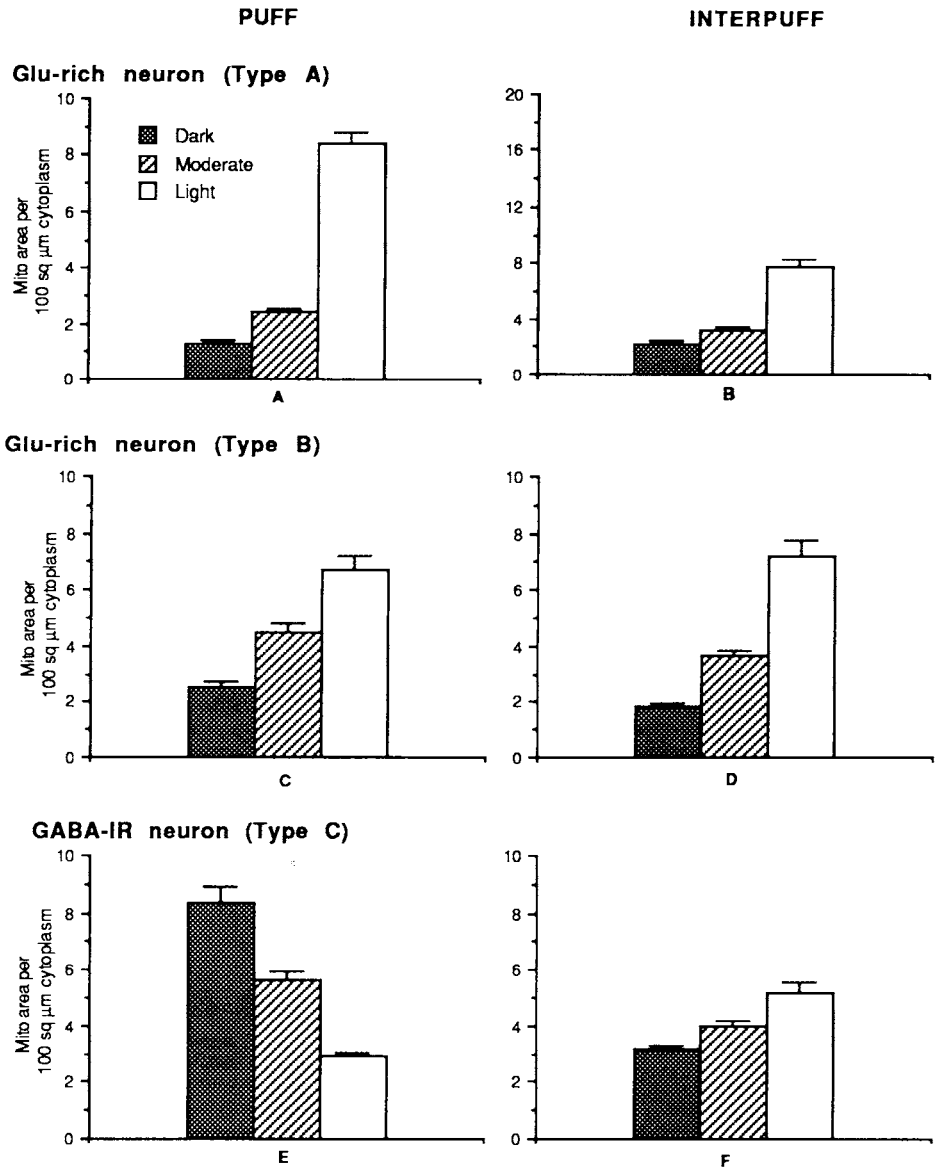

Fig. 11. Areal distribution of mitochondria per 100 μm^2 of cytoplasm in Glu-rich (type A), Glu-rich (type B), and GABA-IR (type C) neurons from puffs (**A,C,E**) and from interpuffs (**B,D,F**). Data are presented as mean values ± S.E.M. According to their CO levels, mitochondria were divided into dark, moderate, and lightly reactive ones. The Glu-rich neurons (A–D) in both regions have a significantly lower proportion of darkly CO-reactive mitochondria than GABA-IR neurons (E–F) ($P < 0.001$). The GABA-IR neurons (E) in puffs have more darkly CO-reactive mitochondria than those interpuffs (F) ($P < 0.001$).

compared to phasically active synapses which contain a lower amount of mitochondria (Atwood and Wojtowicz, 1986; Lnenicka et al. 1986; Shupliakov et al., 1992). These findings suggest that the effects of firing rate in presynaptic axon terminals determine their metabolic levels such that the energy producing capacity is always in excess of current demand. This notion is further supported by the finding that changes in neuronal activity induced by retinal TTX preceded the detectable reduction in CO activity in the monkey striate cortex, indicating that the adjustment of CO levels was in response to the altered presynaptic activity (DeYoe et al., 1995). These and our present findings suggest that more mitochondria with elevated CO levels in Glu-IR terminals in puffs are likely to result from a higher firing rates in these terminals, which place a greater energy demand there. Our present results further suggest that puffs receive more excitatory synapses, which may also be tonically more active, than those in interpuffs. Thus, the correspondence between heightened spiking (spontaneous and evoked) activity and elevated CO levels in puffs (Livingstone and Hubel, 1984a; Wong-Riley and Carroll, 1984; DeYoe et al., 1995) can be accounted for by the present findings that puffs receive a dominant, excitatory drive that is presumed to be largely responsible for maintaining background firing rates. As a result, a greater degree of depolarizing activity in puffs is likely to increase the energy demands and its production through oxidative metabolism, as indicated by a higher CO level in puffs.

Glutamate is reported to be a major excitatory neurotransmitter in the geniculocortical pathway (Ahlsen et al., 1982; Montera and Wenthold, 1989; Montero, 1990; Tsumoto, 1990). Neuroanatomical tracing studies have shown that puffs receive afferent input directly from the lateral geniculate nucleus (LGN) (Livingstone and Hubel, 1982; Fitzpatrick et al., 1983) and are connected reciprocally to adjacent puffs (Livingstone and Hubel, 1984b) as well as to thin CO-rich stripes of the prestriate cortex (Livingstone and Hubel, 1983). On the other hand, interpuffs do not receive direct thalamic input (Livingstone and Hubel, 1982). They are connected reciprocally to neighboring interpuffs (Livingstone and Hubel, 1984b) and they project to CO-poor interstripes of the prestriate cortex (Livingstone and Hubel, 1983). Thus, specific connections of extracortical and intracortical pathways in puffs and interpuffs may constitute the neuroanatomical basis for such a difference in synaptic composition and metabolic activity in presynaptic terminals in the two regions. For instance, Glu-IR axon terminals in puffs, but not in interpuffs, may originate directly from the LGN. Geniculate fibers themselves have a very high level of spontaneous activity and are likely to cause heightened firing rates of puff neurons (Creutzfield and Ito, 1968; Livingstone and Hubel, 1982, 1984a; Simons and Carvell, 1989). As consistent with electrophysiological evidence, thalamocortical terminals in the primary visual cortex of rats have a larger mean size and greater fraction of mitochondria than those of cortical origin, although both types of terminals are Glu-IR (Kharazia and Weinberg, 1994). Thus, it is likely that elevated metabolic and physiological activity in puffs reflects the tonic influences of LGN and, to a lesser extent, the tonic effects of other cortical and subcortical inputs. However, further work is needed to elucidate quantitative differences of Glu-IR axon terminals from different sources to puffs and interpuffs, which can be examined by neuroanatomical tracing methods combined with the present approach.

Functional considerations

One of the most prominent differences in their receptive field properties between puffs and interpuffs lies in a lack of orientation selectivity in cells and neuropil elements of puffs but high orientation selectivity in those of interpuffs (Livingstone and Hubel, 1984a; Ts'o and Gilbert, 1988; Ts'o et al., 1990). The mechanisms underlying such functional diversity is unknown. An excitatory feedforward model proposed by Hubel and Wiesel (1962) postulated that orientation selectivity arises from an appropriate alignment of synaptic input from the LGN, such that geniculate cells whose receptive fields fall along a row excite a cortical cell. However, interpuffs with high orientation selectivity are not found to receive direct geniculate input (Livingstone and Hubel, 1982; Fitzpatrick et al., 1983). In addition, alternative models have invoked orientation-selective geniculate cells (Vidyasagar, 1984, 1987; Shou and Leventhal, 1989). On the other hand, several lines of evidence suggest that the intracortical inhibition mediated mainly by GABA synaptic transmission is involved in the generation of orientation selectivity, such as cross-orientation inhibition (Sillito et al., 1980; Sillito, 1984; Koch and Poggio, 1985; Bolz and Gilbert, 1986; Vidyasagar and Heide, 1986). However, the absence of intracellular IPSPs during stimulation in the nonoptimal orientation argue against major contribution of intracortical inhibition for the generation of orientation selectivity (Ferster, 1987; Ferster and Koch, 1987; Douglas et al., 1989). Thus, no model based on either single excitatory or inhibitory mechanism can explain the generation of orientation selectivity in the visual cortex. Recently, a simulation model called canonical microcircuits suggests that the interaction of excitation and inhibition may play an important role in establishing orientation selectivity and other receptive field properties in the visual cortex (Douglas et al., 1989; Douglas and Martin, 1991; Berman et al., 1992).

Based on the present results and others, we believe that the striking difference in receptive field properties between puffs and interpuffs may depend on their asymmetry of excitatory and inhibitory interactions, such as strength and timing of each to the two regions. First, it can be assumed that there is a stronger excitatory drive in puffs, since they receive more Glu-IR excitatory synapses than interpuffs. Studies on the visual cortex have suggested that the excitatory gain of the cortex may only be modified by a relatively weak intracortical inhibition (Douglas et al., 1989; Douglas and Martin, 1991; Berman et al., 1992). In the face of a strong transient excitation, the inhibitory synaptic mechanisms failed to prevent the excitatory current from producing action potentials, suggesting that the strength of excitatory drive, rather than inhibitory one, plays a dominant role in affecting target cell response (Douglas et al., 1989; Berman et al., 1991, 1992). Furthermore, a nonspecific increase in excitability may allow a cortical cell to respond to almost any stimulus, even the weak, but normally subthreshold ones (Ferster and Koch, 1987; Berman et al., 1992). An increase in the excitability of a cortical cell by intracellular application of Ce^{+}, which blocks K^{+} channels and raises the membrane resistance, can result in spikes being evoked at the nonoptimal orientation (Ferster and Lindstrom, 1983). Thus, the loss of orientation can be accounted for, at least partially, by a nonspecific increase in excitation of a group of cortical cells (e.g., in puffs). In contrast, interpuffs receive relatively weaker excitatory and stronger inhibitory influence than puffs, and may form a basis for their higher orientation selectivity and preference for stimuli of high spatial frequency. However, further work is needed to determine how the interaction of excitation and inhibition is quantitatively correlated with the generation of different receptive field properties. Second, the timing of excitation of puff neurons to retinal stimuli is expected to be earlier than that in interpuffs, because puffs, but not interpuffs, receive direct geniculate input which is considered as an initial driving force for cortical excitation (Livingstone and Hubel, 1982; Fitzpatrick et al., 1983). The excitation provided by the thalamic afferents themselves has to be modified, because it is out of their nonoriented, nondirectional receptive fields that the selective cortical fields are built (Livingstone and Hubel, 1984a; Berman et al., 1992). It has been suggested that cross-orientation inhibition occurring at the visual cortex requires at least a small bias, which could be intracortically generated, to initiate further sharpening of the orientation turning (Sillito, 1979; Worgotter and Koch, 1991). Based on features of delayed excitation and intracortical connection that interpuffs have, we assume that interpuffs may be more likely than puffs to obtain an afferent orientation bias. Consequently, orientation turning could be strengthened substantially with the secondary inhibitory mechanism in interpuffs. However, direct physiological evidence is needed to confirm this possibility.

In conclusion, the present results suggest that the diversities in metabolic activity and physiological properties between puffs and interpuffs may depend on an asymmetry of excitatory and inhibitory interactions in the two regions.

ACKNOWLEDGMENTS

We thank Dr. Peter Somogyi for his generous gift of antisera against GABA. This study was supported by NIH grants EY05439 and NS18122.

LITERATURE CITED

Ahlsen, G., K. Grant, and S. Lindstrom (1982) Monosynaptic excitation of principal cells in the lateral geniculate nucleus by corticofugal fibers. Brain Res. *234:*454–458.

Atwood, H.L. and J.M. Wojtowicz (1986) Short-term and long-term plasticity and physiological differentiation of crustancean motor synapses. In J.R. Smythies and R.J. Bradley (eds): International Review of Neurobiology, Vol 28. New York: Academic Press, pp. 275–362.

Balcar, V.J. and G.A.R. Johnson (1972) The structural specificity of the high affinity uptake of L-glutamate and aspartate by rat brain slices. J. Neurochem. *19:*2657–2666.

Baughman, R.W. and C.D. Gilbert (1980) Aspartate and glutamate as possible neurotransmitters of cells in layer 6 of the visual cortex. Nature *287:*848–850.

Bereiter-Hahn, J. and M. Voth (1983) Metabolic control of shape and structure of mitochondria *in situ*. Biol. Cell *47:*309–322.

Berman, N.J., R.J. Douglas, and K.A.C. Martin (1992) GABA-mediated inhibition in the neural networks of visual cortex. Prog. Brain Res. *90:*443–476.

Berman, N.J., R.J. Douglas, K.A.C. Martin, and D. Whitteridge (1991) Mechanisms of inhibition in cat visual cortex. J. Physiol. *440:*697–722.

Bolz, J. and C.D. Gilbert (1986) Generation of end-inhibition in the visual cortex via interlaminar connections. Nature *320:*362–365.

Broman, J. and O.P. Ottersen (1992) Cervicothalamic tract terminals are enriched in glutamate-like immunoreactivity: An electron microscopic double-labeling study in the cat. J. Neurosci. *12:*204–221.

Carder, R.K. and S.H.C. Hendry (1994) Neuronal characterization, compartmental distribution, and activity-dependent regulation of glutamate immunoreactivity in adult monkey striate cortex. J. Neurosci. *14:*242–262.

Colonnier, M. (1968) Synaptic patterns on different cell types in the different laminae of the cat visual cortex. An electron microscope study. Brain Res. *9:*268–287.

Conti, F. (1991) Toward the anatomical identification of glutamatergic neurons and synapses in the cerebral cortex. In B.S. Meldrum, F. Moroni, R.P. Simon, and J.H. Woods (eds): Excitatory Amino Acids. New York: Raven Press, pp. 45–53.

Conti, F., M. Fabri, and T. Manzoni (1988) Glutamate-positive cortical-cortical neurons in the somatic sensory areas I and II of cats. J. Neurosci. *8:*2948–2960.

Conti, F., J. DeFelipe, I. Farinas, and T. Manzoni (1989) Glutamate-positive neurons and axon terminals in cat sensory cortex: A correlative light and electron microscopic study. J. Comp. Neurol. *290:*141–153.

Cotman, C.W., D.T. Monaghan, O.P. Ottersen, and J. Storm-Mathisen (1987) Anatomical organization of excitatory amino acids receptors and their pathways. Trends Neurosci. *10:*273–280.

Creutzfield, D.D., and M. Ito (1968) Functional synaptic organization of primary visual cortex neurons. Exp. Brain Res. *6:*324–352.

Curtis, D.R. and J.C. Watkins (1963) Acidic amino acids with strong excitatory actions on mammalian neurons. J. Physiol. *166:*1–14.

de Belleroche, J.S. and H.F. Bradford (1972) Metabolism of beds of mammalian cortical synaptosomes: response to depolarizing influences. J. Neurochem. *19:*585–602.

DeYoe, E.A., T.C. Trusk, and M. Wong-Riley (1995) Activity correlates of cytochrome oxidase-defined compartments in granular and supragranular layers of primary visual cortex of the macaque monkey. Vis. Neurosci. *12:*629–639.

Douglas, R.J. and K.A.C. Martin (1991) A functional microcircuit for the visual cortex. J. Physiol. *440:*735–769.

Douglas, R.J., K.A.C. Martin, and D. Whitteridge (1989) A canonical microcircuit for neocortex. Neural Computation *1:*479–487.

Duckrow, R.B., J.C. LaManna, and M. Rosenthal (1981) Direct electrical stimulation of the cerebral cortex suggests that vascular as well as metabolic factors determine the oxidative response. Soc. Neurosci. Abstr. *7:*787.

Erecinska, M. and I.A. Silver (1989) ATP and brain function. J. Cereb. Blood Flow Metab. *9:*2–19.

Erecinska, M. and I.A. Silver (1990) Metabolism and role of glutamate in mammalian brain. Prog. Neurobiol. *35:*245–296.

Ferster, D. (1987) Origin of orientation-selective EPSPs in simple cells of cat visual cortex. J. Neurosci. *7:*1780–1791.

Ferster, D. and C. Koch (1987) Neuronal connections underlying orientation selectivity in cat visual cortex. Trends Neurosci. *10:*487–492.

Ferster, D. and S. Lindstrom (1983) An intracellular analysis of geniculo-cortical connectivity in area 17 of the cat. J. Physiol. *342:*181–215.

Fitzpatrick, D., K. Itoh, and I.T. Diamond (1983) The laminar organization of the lateral geniculate body and the striate cortex in the squirrel monkey (*Saimiri sciureus*). J. Neurosci. *3:*673–702.

Fitzpatrick, D., J.S. Lund, D.E. Schmechel, and A.C. Towles (1987) Distribution of GABAergic neurons and axon terminals in the macaque striate cortex. J. Comp. Neurol. *264:*73–91.

Fonnum, F. (1984) Glutamate: A neurotransmitter in mammalian brain. J. Neurochem. *42:*1–11.

Gray, E.G. (1959) Axo-somatic and axo-dendritic synapses of the cerebral cortex: An electron microscope study. J. Anat. *93:*:420–433.

Hendrickson, A.E., S.P. Hunt, and J.-Y. Wu (1981) Immunocytochemical localization of glutamic acid decarboxylase in monkey striate cortex. Nature *292:*605–607.

Hendry, S.H.C. and R.K. Carder (1992) Organization and plasticity of GABA neurons and receptors in monkey visual cortex. Prog. Brain Res. *22:*477–502.

Hendry, S.H.C. and E.G. Jones (1986) Reduction in number of GABA immunostained neurons in deprived-eye dominance columns of monkey area 17. Nature *320:*750–753.

Hendry, S.H.C., H.D. Schwark, E.G. Jones, and J. Yan (1987) Numbers and proportions of GABA-immunoreactive neurons in different areas of monkey cerebral cortex. J. Neurosci. *7:*1503–1519.

Hendry, S.H.C., J. Fuchs, A.L. de Blas, and E.G Jones (1990) Distribution and plasticity of immunocytochemically localized $GABA_A$ receptors in adult monkey visual cortex. J. Neurosci. *10:*2438–2450.

Hendry, S.H.C., M.M. Huntsman, A. Vinuela, H. Mohler, A.L. de Blas, and E.G. Jones (1994) $GABA_A$ receptor subunit immunoreactivity in primate visual cortex: Distribution in macaques and humans and regulation by visual input in adulthood. J. Neurosci. *14:*2383–2401.

Hertz, L. (1979) Functional interactions between neurons and astrocytes: I. Turnover and metabolism of putative amino acid transmitters. Prog. Neurobiol. *13:*277–323.

Hevner, R.F. and M.T.T. Wong-Riley (1990) Regulation of cytochrome oxidase protein levels by functional activity in the macaque monkey visual system. J. Neurosci. *10:*1331–1340.

Hevner, R.F. and M.T.T. Wong-Riley (1993) Mitochondrial and nuclear gene expression for cytochrome oxidase subunits are disproportionately regulated by functional activity in neurons. J. Neurosci. *13:*1805–1819.

Hicks, T.P. (1987) Excitatory amino acid pathways in cerebral cortex. In T.P. Hicks, D. Lodge, and H. Mclennan (eds): Excitatory Amino Acid Transmission. New York: Alan R. Liss, pp. 373–380.

Hodgson, A.J., B. Penke, A. Erdei, I.W. Chubb, and P. Somogyi (1985) Antiserum to gamma-aminobutyric acid. I. Production and characterization using a new model system. J. Histochem. Cytochem. *33:*229–239.

Hollman, M., A. O'Shea-Greenfield, S.W. Rogers, and S. Heinemann (1989) Cloning by functional expression of a functional glutamate receptor. Nature *342:*643–648.

Hood. D.A. (1990) Co-ordinate expression of cytochrome c oxidase subunit III and VIc mRNAs in rat tissue. J. Biochem. *269:*503–506.

Horton, J.C. and D.H. Hubel (1981) Regular patchy distribution of cytochrome-oxidase staining in primary visual cortex of macaque monkey. Nature *292:*762–764.

Hubel, D.H. and T.N. Wiesel (1962) Receptive fields, binocular interaction and functional architecture in the cat's visual cortex. J. Physiol. *160:*106–154.

Hubel, D.H. and T.N. Wiesel (1969) Anatomical demonstration of columns in the monkey striate cortex. Nature *221:*747–750.

Hubel, D.H. and T.N. Wiesel (1972) Laminar and columnar distribution of geniculocortical fibers in the macaque monkey. J. Comp. Neurol. *146:*421–450.

Kharazia, V. and R.J. Weinberg (1994) Glutamate in thalamic fibers terminating in layer IV of primary sensory cortex. J. Neurosci. *14:*6021–6032.

Koch, C. and T. Poggio (1985) The synaptic veto mechanism: Does it underlie direction and orientation selectivity in the visual cortex? In D. Rose and V.G. Dobson (eds): Models of the visual cortex. New York: John Wiley & Son, pp. 408–419.

Krnjevic, K., and J.K. Phillis (1963) Iontophoretic studies of neurons in the mammalian cerebral cortex. J. Physiol. *165:*274–304.

Kuljis, R.O. and P. Rakic (1989) Neuropeptide Y-containing neurons are situated predominantly outside cytochrome oxidase puffs in macaque visual cortex. Vis. Neurosci. *2:*57–62.

Livingstone, M.S. and D.H. Hubel (1982) Thalamic inputs to cytochrome oxidase-rich regions in monkey visual cortex. Proc. Natl. Acad, Sci. USA *79:*6098–6101.

Livingstone, M.S. and D.H. Hubel (1983) Specificity of cortico-cortical connections in monkey visual cortex. Nature *304:*531–534.

Livingstone, M.S. and D.H. Hubel (1984a) Anatomy and physiology of a color system in the primate visual cortex. J. Neurosci. *4:*309–356.

Livingstone, M.S. and D.H. Hubel (1984b) Specificity of intrinsic connections in primate primary visual cortex. J. Neurosci. *4:*2830–2835.

Lnenicka, G.A., H.L. Atwood, and L. Martin (1986) Morphological transformation of synaptic terminals of a phasic motoneuron by long-term tonic stimulation. J. Neurosci. *6:*2252–2258.

Lowry, O.H. (1975) Energy metabolism in brain and its control. In D.H. Ingvar and N.A. Lassen (eds): Brain Work, Alfred Benzon Symposium, VIII. New York: Academic Press, pp. 48–64.

Lund, J.S. (1990) Excitatory and inhibitory circuitry and laminar mapping strategies in the primary visual cortex of the monkey. In G.M. Edelman, W.E. Gall, and W.M. Cowan (eds): Signal and Sense, Local and Global Order in Perceptual Maps. New York: John Wiley and Sons, pp. 51–66.

Mayer, M.L. and G.L. Westbrook (1987) The physiology of excitatory amino acids in the vertebrate central nervous system. Prog. Neurobiol. *28:*197–276.

Monaghan, D.T., R.J. Bridges, and C.W. Cotman (1989) The excitatory amino acid receptors: Their class, pharmacology, and distinct properties in the function of the central nervous system. Annu. Rev. Pharmacol. Toxicol. *29:*365–402.

Montero, V.M. (1990) Quantitative immunogold analysis reveals high glutamate levels in synaptic terminals of retino-geniculate, corticol-geniculate, and geniculo-cortical axons in the cat. Vis. Neurosci. *4:*437–443.

Montero, V.M. and R.J. Wenthold (1989) Quantitative immunogold analysis reveals high glutamate levels in retinal and cortical synaptic terminals in the lateral geniculate nucleus of the macaque. Vis. Neurosci. *31:*639–647.

Moriyoshi, K., M. Masu, T. Shigemoto, N. Mizuno, and S. Nakanishi (1991) Molecular cloning and characterization of the rat NMDA receptor. Nature *354:*31–37.

Nadler, J.V., W.F. White, K.W. Vaca, D.A. Redburn, and C.W. Cotman (1977) Characterization of putative amino acid transmitter release from slices of rat dentate gyrus. J. Neurochem. *29:*279–290.

Naito, S. and T. Ueda (1983) ATP-dependent uptake of glutamate into protein I-associated synaptic vesicles. J. Biol. Chem. *258:*696–699.

Naito, S. and T. Ueda (1985) Characterization of glutamate uptake into synaptic vesicles. J. Neurochem. *44:*99–109.

Nicholls, D.G. (1989) The release of amino acid neurotransmitters from isolated nerve terminals. J. Neurochem. *52:*331–341.

Nie, F. and M.T.T. Wong-Riley (1995) Double labeling of GABA and cytochrome oxidase in the macaque visual cortex: Quantitative EM analysis. J. Comp. Neurol. *356:*115–131.

Nie, F., R. Curtis, and M. Wong-Riley (1994) Differential distribution of glutamatergic synapses in cytochrome oxidase-rich puffs and -poor interpuffs in primary visual cortex of monkeys. Soc. Neurosci. Abstr. *20:*1578.

Nie, F., E. Godfrey, and M. Wong-Riley (1995) Effect of monocular afferent deprivation on GABAergic neurons in the macaque striate cortex: quantitative EM analysis. Soc. Neurosci. Abstr. in press.

Osen, K., J. Storm-Mathisen, O.P. Ottersen, and B. Dihle (1995) Glutamate is concentrated in and released from parallel fiber terminals in the dorsal cochlear nucleus: A quantitative immunocytochemical analysis in guinea pig. J. Comp. Neurol. *357:*482–500.

Ottersen, O.P. (1989a) Quantitative electron microscopic immunocytochemistry of neuroactive acids. Anat Embryol. *181:*1–15.

Ottersen, O.P. (1989b) Post-embedding immunogold labeling of fixed glutamate: an electron microscopic analysis of relationship between gold particle density and antigen concentration. J. Chem. Neuroanat. *2:*57–66.

Ottersen, O.P., J.H. Laake, and J. Storm-Mathisen (1990) Demonstration of a releasable pool of glutamate in cerebellar mossy and parallel fibre terminals by means of light and electron microscopic immunocytochemistry. Arch. Ital. Biol. *128:*111–125.

Pierce, J.P. and G.R. Lewin (1994) An ultrastructural size principle. Neurosci. *58:*441–446.

Rall, W., R.E. Burke, T.G. Smith, P.G. Nelson, and K. Frank (1967) Dendritic location of synapses and possible mechanisms for the monosynaptic EPSP in motoneurons. J. Neurophysiol. *30:*1169–1193.

Ruscak, M. and R. Whittam (1967) The metabolic response of brain slices to agents affecting the sodium pump. J. Physiol. *19:*595–610.

Shepherd, G.M. (1979) The synaptic organization of the brain. New York: Oxford University Press.

Shou, T. and A.G. Leventhal (1989) Organized arrangement of orientation-selective relay cells in the cat's dorsal lateral geniculate nucleus. J. Neurosci. *9:*4287–4302.

Shupliakov, O., L. Brodin, S. Cullheim, O.P. Ottersen, and J. Storm-Mathisen (1992) Immunogold quantification of glutamate in two types of excitatory synapses with different firing patterns. J. Neurosci. *12:*3789–3803.

Sillito, A.M. (1979) Inhibitory mechanisms influencing complex cell orientation selectivity and their modification at high resting discharge levels. J. Physiol. *289:*33–53.

Sillito, A.M. (1984) Functional considerations of the operation of GABAergic inhibitory processes in the visual cortex. In: E.G. Jones and A. Peter (eds): Cerebral Cortex, Vol. 2. Functional Properties of Cortical Cells. New York: Plenum Press, pp. 91–117.

Sillito, A.M., J.A. Kemp, J.A. Milson, and N. Berardi (1980) A re-evaluation of the mechanisms underlying simple cell orientation selectivity. Brain Res. *194:*517–520.

Simons, D.J. and G.E. Carvell (1989) Thalamocortical response transformation in the rat vibrissa/barrel system. J. Neurophysiol. *61:*311–330.

Somogyi, P. (1989) Synaptic organization of GABAergic neurons and $GABA_A$ receptors in the lateral geniculate nucleus and visual cortex. In D.K-T. Lam and C.D. Gilbert (eds): Neural mechanisms of visual perception. Houston, Texas: Portfolio Pub. Co., pp. 35–62.

Somogyi, P. and I. Soltesz (1986) Immunogold demonstration of GABA in synaptic terminals of intracellularly recorded, horseradish peroxidase-filled basket cells and clutch cells in the cat's visual cortex. Neurosci. *19:*1051–1065.

Somogyi, P., K. Halasy, J. Somogyi, J. Storm-Mathisen, and O.P. Ottersen (1986) Quantification of immunogold labeling reveals enrichment of glutamate in mossy and parallel fibre terminals in cat cerebellum. Neurosci. *19:*1045–1050.

Storm-Mathisen, J. and O.P. Ottersen (1988) Localization of excitatory amino acid transmitters. In D. Lodge (ed): Excitatory Amino Acids in Health and Disease. New York: John Wiley & Son, pp. 107–141.

Storm-Mathisen, J., A.K. Leknes, A.T. Base, J.C. Vaaland, P. Edminson, F.M.S. Haug, and O.P. Ottersen (1983) First visualization of glutamate and GABA in neurons by immunocytochemistry. Nature *301:*517–520.

Toggenburger, G., D. Felix, M. Cuenod, and H. Henke (1982) In vitro release of endogenous beta-alanine, GABA and glutamate, and electrophysiological effect of beta-alanine in pigeon optic tectum. J. Neurochem. *39:*176–183.

Ts'o D.Y. and C.D. Gilbert (1988) The organization of chromatic and spatial interactions in the primate striate cortex. J. Neurosci. *8:*1712–1727.

Ts'o, D.Y., R.D. Frostig, E.E. Lieke, and A. Grinvald (1990) Functional organization of primate visual cortex revealed by high resolution optical imaging. Science *249:*417–420.

Tsumoto, T. (1990) Excitatory amino acid transmitters and their receptors in neural circuits of the cerebral neocortex. Neurosci. Res. *9:*79–102.

Uchizono, K. (1965) Characteristics of excitatory and inhibitory synapses in the CNS of the cat. Nature *207:*642–643.

van den Pol, A.N., J.P. Wuarin, and F.E., Dudek (1990) Glutamate, the dominant excitatory transmitter in neuroendocrine regulation. Science *250:*1276–1278.

Vidyasagar, T.R. (1984) Contribution of inhibitory mechanisms to the orientation sensitivity of cat LGN neurons. Exp. Brain Res. *55:*192–195.

Vidyasagar, T.R. (1987) A model of striate response properties based on geniculate anisotrophies. Biol. Cybern. *57:*11–24.

Vidyasagar, T.R. and W. Heide (1986) The role of GABAergic inhibition in the response properties of neurons in cat visual area 18. Neurosci. *17:*49–55.

Watkins, J.C. and R.H. Evans (1981) Excitatory amino acid transmitter. Annu. Rev. Pharmacol. Toxicol. *21:*165–204.

Wikstrom, M., K. Krab, and M. Saraste (1981) Cytochrome Oxidase: A Synthesis. New York: Academic Press.

Williams, R.S., M. Garcia-Moll, J. Mellor, S. Salmons, and W. Harlan (1987) Adaption of skeletal muscle to increased contractile activity: Expression of nuclear genes encoding mitochondrial proteins. J. Biol. Chem. *262:* 2764–2767.

Wong-Riley, M.T.T. (1979) Changes in the visual system of monocularly sutured or enucleated cats demonstrable with cytochrome oxidase histochemistry. Brain Res. *171:*11–28.

Wong-Riley, M.T.T. (1989) Cytochrome oxidase: An endogenous metabolic marker for neuronal activity. Trends Neurosci. *12:*94–101.

Wong-Riley, M.T.T. (1994) Dynamic metabolic organization and plasticity revealed by cytochrome oxidase. In A. Peters and K.S. Rockland (eds): Primate Visual Cortex. Cerebral Cortex. Vol. 10. New York: Plenum Press, pp. 141–200.

Wong-Riley, M. and E.W. Carroll (1984) The effect of impulse blockage on cytochrome oxidase activity in the monkey visual system. Nature *307:*262–264.

Wong-Riley, M.T.T., S.C. Tripathi, T.C. Trusk, and D.A. Hoppe (1989a) Effect of retinal impulse blockage on cytochrome oxidase-rich zones in the macaque striate cortex: I. Quantitative EM analysis of neurons. Vis. Neurosci. *2:*483–497.

Wong-Riley, M.T.T., T.C. Trusk, S.C. Tripathi, and D.A. Hoppe (1989b) Effect of retinal impulse blockade on cytochrome oxidase-rich zones in the macaque striate cortex: II. Quantitative EM analysis of neuropil. Vis. Neurosci. *2:*499–514.

Wong-Riley, M.T.T., T. Trusk, W. Kaboord, and Z. Huang (1994) Effect of retinal impulse blockage on cytochrome oxidase-poor interpuffs in the macaque striate cortex: quantitative EM analysis of neurons. J. Neurocytol. *23:*533–553.

Worgotter, F. and C. Koch (1991) A detailed model of the primary visual pathway in the cat: Comparison of afferent excitatory and intracortical inhibitory connection schemes for orientation selectivity. J. Neurosci. *11:*1959–1979.

Wuarin, J.P. and F.E. Dudek (1991) Excitatory amino acid antagonists inhibit synaptic response in the guinea pig hypothalamic paraventricular nucleus. J. Neurophysiol. *65:*946–951.